

---

Masters Theses

Student Theses and Dissertations

---

Fall 2012

## Transport of a methamphetamine surrogate through painted drywall and accumulation in insulation

Nishanthini Vijayakumar Shakila

Follow this and additional works at: [https://scholarsmine.mst.edu/masters\\_theses](https://scholarsmine.mst.edu/masters_theses)

 Part of the [Civil and Environmental Engineering Commons](#)

Department:

---

### Recommended Citation

Vijayakumar Shakila, Nishanthini, "Transport of a methamphetamine surrogate through painted drywall and accumulation in insulation" (2012). *Masters Theses*. 7080.

[https://scholarsmine.mst.edu/masters\\_theses/7080](https://scholarsmine.mst.edu/masters_theses/7080)

This thesis is brought to you by Scholars' Mine, a service of the Missouri S&T Library and Learning Resources. This work is protected by U. S. Copyright Law. Unauthorized use including reproduction for redistribution requires the permission of the copyright holder. For more information, please contact [scholarsmine@mst.edu](mailto:scholarsmine@mst.edu).

**TRANSPORT OF A METHAMPHETAMINE SURROGATE THROUGH PAINTED  
DRYWALL AND ACCUMULATION IN INSULATION**

**by**

**NISHANTHINI VIJAYAKUMAR SHAKILA**

**A THESIS**

**Presented to the Faculty of the Graduate School of the  
MISSOURI UNIVERSITY OF SCIENCE AND TECHNOLOGY**

**In Partial Fulfillment of the Requirements for the Degree**

**MASTER OF SCIENCE IN ENVIRONMENTAL ENGINEERING**

**2012**

**Approved by**

**Glenn C. Morrison, Advisor  
Joel G. Burken  
Douglas K. Ludlow**

© 2012

Nishanthini Vijayakumar Shakila

All Rights Reserved

## ABSTRACT

Methamphetamine is a drug of abuse in the United States and it is frequently produced in residential “meth labs”. During a specific cooking stage called “salting out”, a high concentration of methamphetamine is released into the air and can accumulate on and within indoor surfaces. Even after remediation, methamphetamine and other chemicals can be released into the occupied space by diffusion and desorption from insulation and painted drywall. To better understand the emission characteristics of methamphetamine, the diffusion coefficient of n- isopropylbenzylamine (NIBA; an isomer and surrogate for methamphetamine) was measured in latex painted drywall. To quantify the diffusion coefficient, the flux of NIBA through a painted drywall specimen was measured using a modified “cup method” and a flow-through chamber. Water was used as a control to validate the method. The steady state effective diffusion coefficient of NIBA for painted drywall was found to be  $2.1 \pm 1.4 \times 10^{-7} \text{ m}^2/\text{sec}$  and the estimated effective diffusion coefficient of paint was  $3.0 \times 10^{-9} \text{ m}^2/\text{sec}$ . Also measured was the partition coefficient of NIBA to two different types of cavity insulation. Accumulation and release of methamphetamine was simulated using a mass balance model of wall cavities and an entire house. For an illegal lab that operates continuously for 2 weeks in a small house, greater than 10 grams of methamphetamine can accumulate behind walls in the cavity insulation. It would require several months to years to deplete this reservoir if the accumulated methamphetamine is emitted at rates resulting in “safe” indoor concentrations. During the initial period following the cooking activity the daily dose for an adult can start as high as  $120 \mu\text{g}/\text{kg}/\text{day}$  and decreases for months until it reaches a safe dose.

## ACKNOWLEDGEMENTS

Thanks to Dr.Morrison for giving me an opportunity to work in the project and his support and help to finish the research and thesis.

Thanks to NIST for funding the research

Thanks to Dr.Burken and Dr.Ludlow for assistance as committee members.

Thanks to Dr.Honglan, Dr.Shu Shi and Garry Abbott for helping me with the analytical instruments.

Thanks to all my friends in the department for their help during my research.

Thanks to my parents and friends for supporting me and encouraging me throughout the degree program.

## TABLE OF CONTENTS

	Page
ABSTRACT.....	iii
ACKNOWLEDGEMENTS.....	iv
LIST OF ILLUSTRATIONS.....	ix
LIST OF TABLES.....	xi
1. INTRODUCTION.....	1
1.1. BACKGROUND.....	1
1.2. HEALTH EFFECTS AND REFERENCE DOSE FOR METHAMPHETAMINE.....	1
1.3. METHAMPHETAMINE PROPERTIES.....	2
1.4. METHAMPHETAMINE MANUFACTURE.....	3
1.4.1. Red phosphorous method.....	4
1.4.2. Birch reduction.....	4
1.4.3. Emde method.....	5
1.4.4. P2P method.....	6
1.4.5. One pot method.....	6
1.5. TRENDS IN ILLICIT METHAMPHETAMINE PRODUCTION.....	6
1.6. METHAMPHETAMINE IN INDOOR ENVIRONMENTS.....	7
1.6.1. Accumulation of methamphetamine in building materials during the cooking process.....	7
1.6.2. Air concentration of methamphetamine during synthesis.....	8
1.7. REMEDIATION GUIDELINES AND REGULATIONS FOR METHAMPHETAMINE CONCENTRATIONS INDOORS.....	8
1.8. PERSISTANCE OF METHAMPHETAMINE IN LATEX PAINTED DRYWALL.....	9
1.9. MECHANISMS OF ACCUMULATION AND TRANSPORT OF ORGANIC COMPOUNDS IN BUILDING MATERIALS.....	10
1.10. MEASUREMENT OF THE EFFECTIVE DIFFUSION COEFFICIENT AND PARTITION COEFFICIENT.....	12
1.10.1. Measuring effective diffusion coefficient ( $D_e$ ).....	12
1.10.2. Measuring partition coefficient (K).....	13

1.11. BOX MODEL TO PREDICT INDOOR METHAMPHETAMINE CONCENTRATION .....	14
1.12. WALL ASSEMBLY OF A BUILDING AND METHAMPHETAMINE CONTAMINATION .....	16
1.13. PURPOSE OF RESEARCH.....	17
2. GOALS AND OBJECTIVES .....	19
2.1. OBJECTIVE 1: MEASURE THE EFFECTIVE DIFFUSION COEFFICIENT OF PAINTED DRYWALL .....	19
2.2. OBJECTIVE 2: MEASURE THE PARTITION COEFFICIENT OF METHAMPHETAMINE IN INSULATION.....	19
2.3. OBJECTIVE 3: ESTIMATE THE ACCUMULATION AND THE RESULTING METHAMPHETAMINE AIR CONCENTRATION DUE TO REEMISSION.....	20
2.4. OBJECTIVE 4: ESTIMATE THE ACCUMULATED METHAMPHETAMINE DOSE FOR ADULTS AND CHILDREN AND THE TIME REQUIRED TO REACH A SAFE INDOOR CONCENTRATION .....	20
3. MATERIALS AND METHODS .....	21
3.1. MATERIALS.....	21
3.1.1. Building materials. ....	21
3.1.2. N- isopropylbenzylamine. ....	21
3.1.3. Toluene. ....	21
3.1.4. Insulation. ....	21
3.1.5. SPME fibers.....	21
3.1.6. HOBO data logger.....	21
3.2. EXPERIMENTAL METHODS.....	22
3.2.1. Objective 1. ....	22
3.2.1.1 Apparatus and procedure used for determining the diffusion coefficient for building material. ....	22
3.2.1.1.1 Diffusion vessel/reaction flask.....	23
3.2.1.1.2 Outer flow-through chamber.....	24
3.2.1.1.3 Sampling procedure and steady state concentration $C_{out}$ . ....	24
3.2.1.1.4 Equations to calculate $D_e$ . ....	24

3.2.1.2 Apparatus used to generate a low concentration (ppb) standard for the diffusion experiment. ....	25
3.2.1.2.1 SPME/GC/MS.....	27
3.2.1.2.2 Calibration procedure.....	27
3.2.1.3 Apparatus used as a high concentration (ppm) standard for diffusion experiment.....	27
3.2.1.3.1 Calibration procedure.....	28
3.2.1.4 Measuring the diffusion coefficient of water in samples U3 and P2.....	28
3.2.1.4.1 Procedure for calculating diffusion coefficient using water vapor permeability values in gypsum board and painted gypsum boards. ....	29
3.2.1.5 Apparatus used for measuring vapor pressure of NIBA. ....	30
3.2.1.5.1 TENAX/FID. ....	31
3.2.1.5.2 Sampling procedure and calibration. ....	31
3.2.1.5.3 SPME calibration for pure NIBA. ....	32
3.2.1.5.4 SPME/GC/MS.....	32
3.2.1.6 Measuring the Saturation concentration beneath the sample in diffusion experiment. ....	33
3.2.1.7 Toluene contamination elimination .....	33
3.2.2. Objective 2. ....	34
3.2.2.1 Experimental procedure. ....	34
3.2.3. Objective 3 and 4.....	35
3.2.3.1 Dynamic approach for accumulation of methamphetamine through drywall during a two week cooking process. ....	36
3.2.3.1.1 Phase 1: Accumulation .....	36
3.2.3.1.2 Phase 2: Reemission of methamphetamine into building.....	38
3.2.3.1.3 Daily methamphetamine intake and cumulative exposure. ....	40
4. RESULTS.....	42
4.1. NIBA MEASUREMENTS AND CALIBRATIONS .....	42
4.1.1. Effective diffusion coefficient ( $D_e$ ). ....	42
4.1.2. Emission rates from gas phase standard systems. ....	44
4.1.3. Calibrating SPME for low range diffusion system. ....	45



4.1.4. Calibrating SPME for high range diffusion system. ....	46
4.1.5. Validating the setup using diffusion of water. ....	47
4.1.6. NIBA - drywall chemistry. ....	48
4.1.7. Vapor pressure of pure NIBA. ....	49
4.1.8. Saturation concentration beneath the drywall. ....	51
4.1.9. Partition coefficient in insulation. ....	51
4.2. MODELLING THE ACCUMULATION AND DECAY PHASE OF METHAMPHETAMINE INDOORS .....	52
4.2.1. Accumulation phase. ....	53
4.2.2. Release phase. ....	54
4.2.3. Daily intake due to inhalation. ....	56
4.2.4. Cumulative dose. ....	59
5. CONCLUSIONS AND PRACTICAL IMPLICATIONS .....	60
5.1. SUMMARY OF EXPERIMENTAL RESULTS .....	60
5.2. PRACTICAL IMPLICATIONS .....	60
5.3. CONCLUSIONS .....	61
6. FUTURE RESEARCH .....	63
6.1. BUILDINGS AND BUILDING MATERIALS .....	63
6.2. CHEMISTRY OF BUILDING MATERIALS .....	63
6.3. DIFFUSION EXPERIMENTS AT LOWER CONCENTRATIONS .....	63
APPENDIX .....	64
BIBLIOGRAPHY .....	92
VITA .....	96

## LIST OF ILLUSTRATIONS

Figure	Page
Figure 1.1. Methamphetamine production by Red phosphorous method.....	4
Figure 1.2. Methamphetamine production by Birch method.....	5
Figure 1.3. Methamphetamine production by Emde method .....	6
Figure 1.4. Bar graph showing the increase in meth labs from year 2007 to 2010.....	7
Figure 1.5. Box model to estimate the concentration of methamphetamine in a well-mixed house.....	17
Figure 1.6. Three different types of wall assemblies with vapor barrier on the exterior side .....	17
Figure 3.1. Apparatus showing diffusion setup .....	23
Figure 3.2a & 3.2b. Shows the drywall and glass pyrex diffusion flask .....	23
Figure 3.3. Experimental apparatus for low range calibration.....	25
Figure 3.4. Experimental setup for high range calibration .....	27
Figure 3.5. Saturator – Tenax TA apparatus for measuring vapor pressure .....	30
Figure 3.6. Measuring concentration beneath the drywall sample .....	32
Figure 3.7. Showing the stainless steel needle inserted into the sample.....	33
Figure 3.8. Measuring the weight gain in insulation .....	35
Figure 3.9. Accumulation and release of methamphetamine behind the wall assembly .....	36
Figure 4.1. Dynamic concentration profile inside the flow through chamber .....	43
Figure 4.2. Mass of NIBA in V1 vs time.....	44
Figure 4.3. Mass of NIBA in V2 vs time.....	45
Figure 4.4. GCMS SCAN-mode response for low-concentration ( $84 \pm 12$ ppb) calibration system.....	46
Figure.4.5. GCMS SCAN-mode response for high-concentration ( $406 \pm 19$ ppb) calibration system.....	47
Figure 4.6. Reaction mechanisms from imines to carbonyls .....	48
Figure 4.7. Response for benzaldehyde using SPME.....	49
Figure 4.8. Peak area vs volume injected from saturator.....	50
Figure 4.9. Peak area vs mass injected from dynacalibrator.....	50

Figure 4.10. Partition coefficients for 10% NIBA equilibration .....	52
Figure 4.11. Simulated accumulation in cellulose insulation for a period of two weeks operation .....	53
Figure 4.12. Simulated accumulation in fiber glass insulation for two weeks operation .....	54
Figure 4.13. Simulated concentrations in room due to emissions from cellulose insulation through drywall.....	55
Figure 4.14. Shows the decay phase due to fiberglass installation.....	56
Figure 4.15. Daily dose due emissions from unpainted drywall and cellulose insulation .....	57
Figure 4.16. Daily dose due to emissions from painted drywall and cellulose insulation .....	57
Figure 4.17. Daily dose due to emissions from unpainted drywall and fiberglass insulation.....	58
Figure 4.18. Daily dose due to emissions from painted drywall and fiber glass insulation.....	58

## LIST OF TABLES

Table	Page
Table 1.1. Properties of methamphetamine and its surrogate NIBA .....	3
Table 3.1. Shows the assumptions to calculate the daily inhalation intake .....	40
Table 4.1. Steady state flux and effective diffusion coefficient for drywall and painted drywall samples.....	43
Table 4.2. Comparison of low range and high range system.....	44
Table 4.3. Tabulated values of diffusion coefficients of water in literature and actual experiment.....	48
Table 4.4. Equilibrium partition coefficient $K'$ .....	51
Table 4.5. Methamphetamine accumulation in insulation .....	53
Table 4.6. Time required to reduce indoor concentrations to safe levels during the release phase .....	55
Table 4.7. Cumulative dose of methamphetamine during reemission period.....	59
Table A1. Showing the dynamic $C_{out}$ in flow through chamber for NIBA in sample U1 .....	65
Table A2. Showing the estimated $D_e$ for NIBA in sample U1 .....	65
Table A3. Showing the dynamic $C_{out}$ in flow through chamber for NIBA in sample P1 .....	66
Table A4. Showing the estimated $D_e$ for NIBA in sample P1 .....	66
Table A5. Showing the dynamic $C_{out}$ in flow through chamber for NIBA in sample U3 .....	67
Table A6. Showing the estimated $D_e$ for NIBA in sample U3 .....	67
Table A7. Showing the dynamic $C_{out}$ in flow through chamber for NIBA in sample P2 .....	68
Table A8. Showing the estimated $D_e$ for NIBA in sample P2.....	68
Table A9. Showing the dynamic $C_{out}$ in flow through chamber for water in sample U3 .....	69
Table A10. Showing the estimated $D_e$ based on literature values for water in sample U3 .....	69
Table A11. Showing the estimated $D_e$ from experiment using water for sample U3.....	70
Table A12. Showing the dynamic $C_{out}$ in flow through chamber for water in sample P2 .....	71

Table A13. Showing the estimated $D_e$ based on literature values for water in sample P2 .....	71
Table A14. Showing the estimated $D_e$ from experiment using water for sample P2 .....	72
Table A15. Mass change of NIBA in Vial V1 .....	73
Table A16. Emission rate of NIBA in Vial V1 .....	73
Table A17. Mass change of NIBA in Vial V2 .....	74
Table A18. Mass change of NIBA in Vial V2 .....	74
Table A20. Volume response for Saturator in FID .....	75
Table A21. Mass response from dynacalibrator .....	76
Table A22. Calculation of vapor pressure from saturation experiment .....	76
Table A23. Saturation concentration beneath the sample U1 .....	77
Table A24. Saturation concentration beneath the sample P1 .....	77
Table A25. Density of insulation .....	78
Table A26. Partition coefficient of NIBA in fiber glass insulation .....	79
Table A27. Partition coefficient of NIBA in cellulose insulation .....	79
Table A28. Showing the parameters for accumulation model, sample U1, in cellulose .....	80
Table A29. Showing accumulation model sample U1 in cellulose insulation .....	80
Table A30. Showing the parameters for accumulation model sample P1, in cellulose .....	81
Table A31. Showing accumulation model sample P1 in cellulose insulation .....	81
Table A32. Showing the parameters for re emission model sample U1 in cellulose .....	82
Table A33. Showing reemission for sample U1 in cellulose insulation .....	82
Table A34. Showing the parameters for re emission model sample P1 in cellulose .....	83
Table A35. Showing reemission for sample P1 in cellulose insulation .....	83
Table A36. Showing the parameters for accumulation model sample U1 in fiberglass .....	84
Table A37. Showing accumulation model sample U1 in fiberglass .....	84
Table A38. Showing the parameters for accumulation model sample P1 in fiberglass .....	85

Table A39. Showing accumulation model sample P1 in fiberglass.....	85
Table A40. Showing the parameters for re emission model sample U1 due to fiberglass.....	86
Table A41. Showing reemission for sample U1, in fiberglass insulation.....	86
Table A42. Showing the parameters for re emission model sample P1 due to fiberglass.....	87
Table A43. Showing reemission for sample P1 in fiberglass insulation .....	87
Table A44. Daily intake due to inhalation for cellulose insulation and sample P1 .....	88
Table A45. Daily intake due to inhalation for cellulose insulation and sample U1 .....	89
Table A46. Daily intake due to inhalation for fiberglass insulation and sample U1 .....	90
Table A47. Daily intake due to inhalation for fiberglass insulation and sample P1.....	91

## **1. INTRODUCTION**

### **1.1. BACKGROUND**

Methamphetamine (meth) is an illegal drug, a substituted amphetamine, and central nervous system stimulant. Meth was first synthesized to treat medical conditions, including attention deficit disorder, obesity, and fatigue (Hunt, Kuck & Truitt, 2006). Due to its strong stimulant effect, meth has become a drug of abuse which can cause neurological damage to heavy users (Hunt et al., 2006). Methamphetamine is relatively easy to synthesize in illegal laboratories (meth labs) using materials such as cold medications and solvents. These meth labs have been found in houses, apartments, hotel rooms and vehicles, and contamination with hazardous chemicals is common (Colorado Department of Public Health and Environment [CDPHE] 2003; Roxanna ZW et al., 2007) Methamphetamine itself contaminates indoor environments through spills and as it evaporates into the air during synthesis, also known as a “cook” (Martyny JW, et al., 2007) (Martyny JW, et al., 2009). Thus synthesis can result in high concentrations of methamphetamine in indoor air and also on the surfaces of the building materials (Martyny JW, et al., 2007 ;Martyny JW, et al., 2009). Methamphetamine can also penetrate into paint and potentially into other materials by diffusion (Martyny et al., 2008; Minnesota Pollution Control Agency, 2007). This legacy methamphetamine can later be released into the building air, resulting in increased exposure for new occupants. To better understand the impact of legacy methamphetamine on future occupants of former meth labs, methamphetamine transport through drywall was studied. Specifically, the effective diffusion coefficient of N-Isopropylbenzylamine (NIBA), a surrogate for meth, was measured. The effective diffusivity of methamphetamine through drywall can be used to make predictions about the rate and extent of accumulation during illegal meth activity, and also the rate of emissions during reoccupation.

### **1.2. HEALTH EFFECTS AND REFERENCE DOSE FOR METHAMPHETAMINE**

Methamphetamine is prescribed as medicine to treat attention deficit disorder (ADHD) in children under the name DESOXYN (Tracy LH et al, 2006). The prescribed amount is

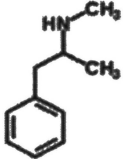
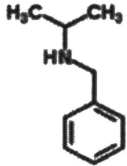
about 5 - 25 mg/day (Tracy LH et al, 2006). This results in a dose of 0.23 – 1.15 mg/kg/day for a child and 0.07 – 0.3 mg/kg/day for an adult female (Tracy LH et al, 2006). The symptoms for this dose include anxiety, difficulty falling asleep and eating disorders (Tracy LH et al, 2006). CNS stimulation, mydriasis (dilation of pupils), anorexia, tachycardia (rapid heart rate) and hypertension are some of the health effects of exposure to methamphetamine (Salocks CB, 2009). A reference dose (RfD) of 0.3 µg/kg/day has been proposed as a risk based standard based on numerous studies of methamphetamine use in adults and children. The reference dose of 0.3 µg/kg/day is specifically based on an observed LOAEL (lowest observable adverse effect level) of 0.08 mg/kg/day in women (Chapman, 1961) and a safety factor of 300 that accounts for deficiencies in toxicity database, inter-individual variation insensitivity and a conversion to a NOAEL (no observable adverse effect level)(Salocks, 2009). This reference dose, and a corresponding maximum air concentration, will be compared against predictions of indoor concentrations that result from dynamics of methamphetamine accumulation and decay of methamphetamine from walls. To put this RfD in perspective for inhalation dose, a 25 kg child breathing 15 m<sup>3</sup> per day will inhale the reference dose in 24 hours if the air concentration is 0.5 µg/m<sup>3</sup> (0.08 ppb).

### **1.3. METHAMPHETAMINE PROPERTIES**

The IUPAC name for meth is N-benzylpropan-2-amine. Shown in Table 1.1 are the chemical structure and known or predicted properties. Meth is a controlled drug, hence its surrogate, N-isopropylbenzylamine (NIBA) was used in the diffusion experiments. NIBA is an isomer with similar physical properties as meth, and is used to dilute meth by methamphetamine manufacturers (Sanderson RS, 2008).



Table 1.1. Properties of methamphetamine and its surrogate NIBA

Properties	Methamphetamine	NIBA
Formula	C <sub>10</sub> H <sub>15</sub> N	C <sub>10</sub> H <sub>15</sub> N
Structure	 Source: Chemspider.com	 Source: Chemspider.com
Molecular weight (g/mol)	149.23	149.23
Polarizability (cm <sup>3</sup> ) <sup>a</sup>	19.27	19.27
Vapor pressure (mmHg at 25°C)	0.147	0.332
Boiling point ( at 760 mmHg) <sup>a</sup>	215°C	200°C
Log (octanol-water partition coefficient, P) <sup>a</sup>	1.94	2.40
Log (octanol-air partition coefficient, K <sub>oa</sub> ) <sup>b</sup>	6.08	5.84
Molar volume (cm <sup>3</sup> ) <sup>a</sup>	164.4	164.4

a. Predicted value from chemspider.com

b. Predicted by EPA Suite.

#### 1.4. METHAMPHETAMINE MANUFACTURE

Hunt et al., (2006) state that meth that is used in the US is most often produced in the US or in Mexico. Meth may either be produced in “small labs making only a few pounds at a time or in super labs which produce 10 pounds or more in production cycle”. Different types of illicit methamphetamine production include,

- Red phosphorous method,
- Nazi or birch method,
- Emde method
- Phenyl – 2 – Propanone (P2P) method,
- One pot method.

**1.4.1. Red phosphorous method.** In this method, red phosphorous (a match box striker chemical), and iodine (obtained from disinfectant solutions) are reacted to form hydroiodic acid (Salocks et.al, 2003). Ephedrine or pseudoephedrine (from cold and cough medicines) is then reacted with the hydroiodic acid (Cantrell TS, et.al, 1980). The reaction mixture is then filtered, basified and extracted into a solvent (United Nations Office on Drugs and Crimes [UNODC], 2006). Meth oil is then formed and hydrogen chloride gas is passed through the oil to convert the methamphetamine into its hydrochloride salt (UNODC, 2006).

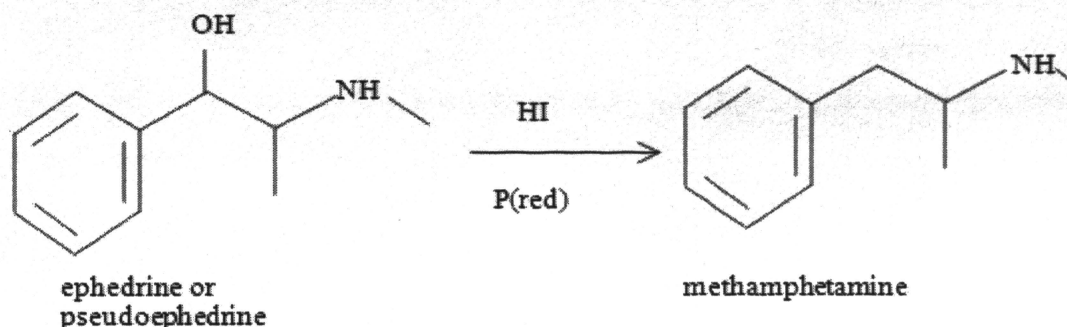


Figure 1.1. Methamphetamine production by Red phosphorous method

**1.4.2. Birch reduction.** In this method ephedrine or pseudoephedrine is dissolved in a metal solution (sodium or lithium) and anhydrous ammonia gas (from fertilizer) is passed through the solution followed by meth oil extraction (UNODC, 2006). Since the process involves anhydrous ammonia, explosions are common.

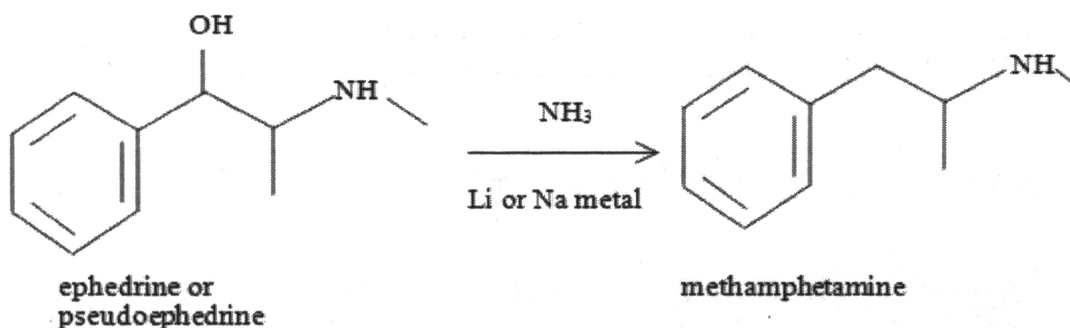
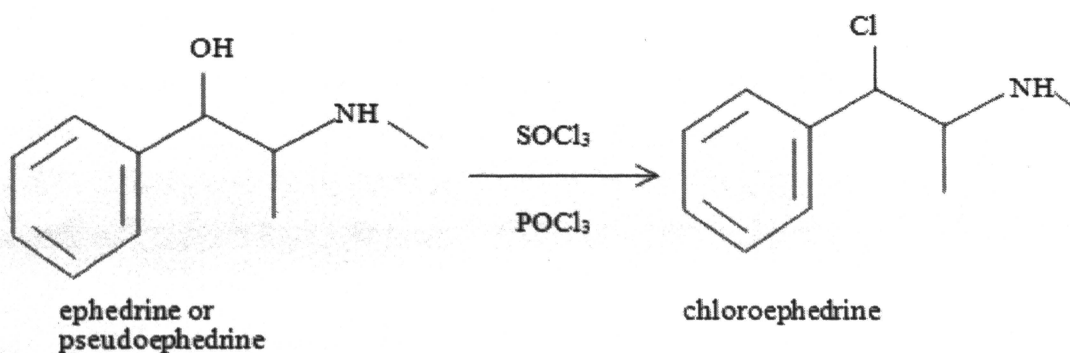


Figure 1.2. Methamphetamine production by Birch method

**1.4.3. Emde method.** In this method when ephedrine or pseudoephedrine is reacted with thionylchloride, it results in the formation of chloroephedrine (UNODC, 2006). The reacting mixture is then hydrogenated with either a platinum or palladium catalyst to form methamphetamine (UNODC, 2006).



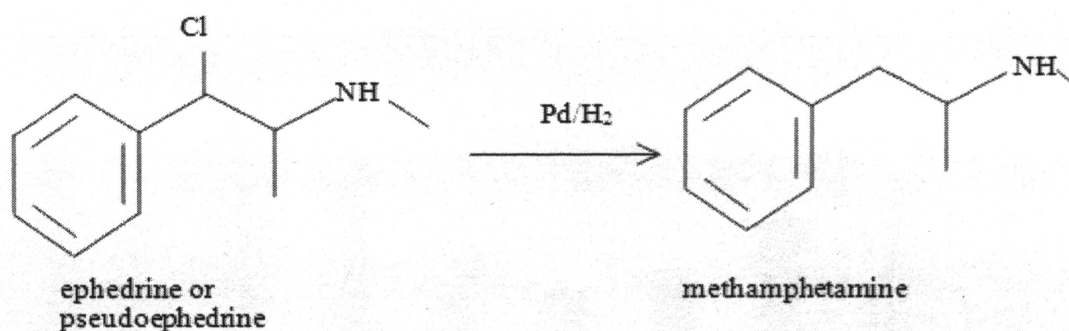


Figure 1.3. Methamphetamine production by Emde method

**1.4.4. P2P method.** This is one of the oldest methods used by the motorcycle gangs (Owen Frank, 2007, pp 17-18). In the P2P method, reductive amination of phenylacetone with methylamine initiates the synthesis. Aluminum (from aluminum foil) and mercury amalgam are used as a reducing agents to produce methamphetamine.

**1.4.5. One pot method.** The one pot method is a recent development and is used to produce a very small quantity of methamphetamine. This method utilizes the same ingredients as the Birch method uses, where all contents are usually mixed and reacted together in a small plastic two liter container (United States Department of Justice, [USDJ] 2010). The mixture then produces ammonia. This ammonia reacts with pseudoephedrine in the presence of lithium to produce methamphetamine (USDJ, 2010).

## 1.5. TRENDS IN ILLICIT METHAMPHETAMINE PRODUCTION

The United States Drug Enforcement Administration [USDEA] reported an increasing trend in total meth clandestine labs, dumpsites and chemical/glass/equipment (USDEA, 2010). While still below historical highs, the number of clandestine meth lab seizures has increased since 2007. In 2010, the largest number of seizures (1,917) was in the state of Missouri. (USDEA, 2010).

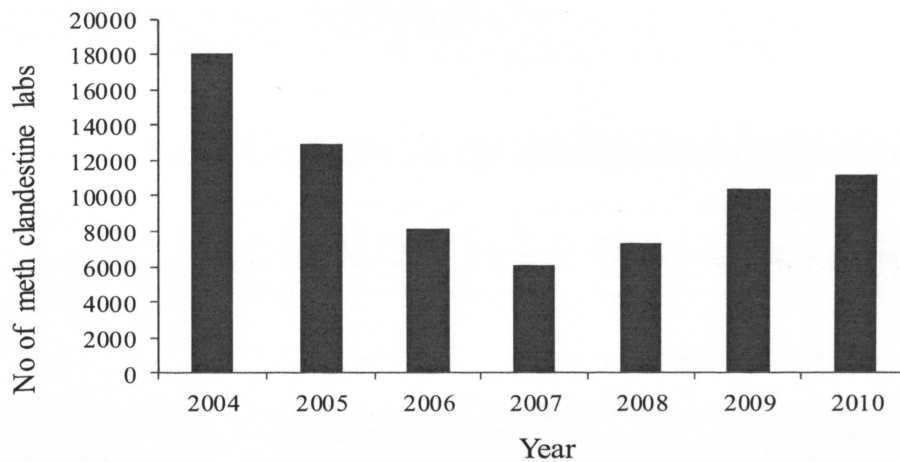


Figure 1.4. Bar graph showing the increase in meth labs from year 2007 to 2010

In addition to the meth labs that have been reported, a large number of unidentified labs add to the risk of exposure to methamphetamine to individuals occupying a former meth house.

## 1.6. METHAMPHETAMINE IN INDOOR ENVIRONMENTS

**1.6.1. Accumulation of methamphetamine in building materials during the cooking process.** During methamphetamine synthesis hydrogen chloride gas is passed through a solvent containing free-base methamphetamine. This acid-base reaction results in crystals of methamphetamine hydrochloride. Bubbles are released from the solution and burst, generating small aerosols (droplets or crystals) containing methamphetamine. These aerosols contaminate floors, walls and any materials present in the room and house (Martyny JW, et al., 2007). During a controlled cooking operation inside a test house, the vertical and horizontal surfaces of the house were tested for methamphetamine using wipe samples (Martyny JW, et al., 2007). Vertical surfaces had  $20 \mu\text{g}/100 \text{ cm}^2$  of methamphetamine contaminating it (Martyny JW, et al., 2007); this was probably mostly in the salt form. In a separate experiment, meth smoking was simulated and walls collected about  $0.1$  to  $5 \mu\text{g}/100 \text{ cm}^2$  of methamphetamine (Martyny

JW, et al., 2008). Explosions in labs are also common (Santos A.P, et al., 2004). A wipe sample of the ceiling of the lab that had experienced an explosion collected 16000  $\mu\text{g}/100\text{ cm}^2$  of methamphetamine (Martyny JW, et al., 2008).

**1.6.2. Air concentration of methamphetamine during synthesis.** Very few measurements of methamphetamine air concentrations have been collected in laboratory or field studies. Air samples collected during a simulated salting-out process resulted in between 79 and 5500  $\mu\text{g}/\text{m}^3$  of methamphetamine (Martyny JW, et al., 2007) (Martyny JW, et al., 2008). Because the chloride salt is formed during salting out, most of the sample is likely to be in the salt form. However, the widespread use of ammonia for methamphetamine synthesis is likely to convert the salt to the free-base form. This could account for the large amount of methamphetamine found dissolved in paint samples (Martyny JW, et al., 2009) and the subsequent release into air after a lab has been dismantled. Air sampling from a methamphetamine lab showed that the airborne methamphetamine concentration was in the 0.1  $\mu\text{g}/\text{m}^3$  range, 3 months after the site was shut down (Minnesota pollution control agency, MPCA, Delavan, 2005).

## **1.7. REMEDIATION GUIDELINES AND REGULATIONS FOR METHAMPHETAMINE CONCENTRATIONS INDOORS**

According to the cleanup guidelines set up by the EPA in 2008, when a meth lab is identified, bulk chemicals, contaminated items such as carpet, furniture, clothes, and surfaces with obvious stains should be removed immediately. After this, the guidelines suggest airing out, removing fiberglass insulation, HEPA vacuuming and/or washing surfaces, removing the dust in the HVAC system and changing filters (United States Environment Protection Agency (USEPA), 2008). Detergent solution wash is recommended for cleaning walls and ceilings (USEPA, 2008). Most of the volatile organic compounds are removed by direct removal (e.g. bottles) and ventilating the building. Non-volatile materials are removed directly (e.g. sodium metal in containers) and by vacuuming dust. The final clean-up standard is based on the level of surface contamination of methamphetamine itself. The EPA and most of the states have established voluntary methamphetamine lab clean-up guidelines which require or recommend that the surface concentration of methamphetamine should meet a certain standard. These standards are in the range of

0.05  $\mu\text{g}/100\text{cm}^2$  to 0.5  $\mu\text{g}/100\text{cm}^2$ , typically 0.1  $\mu\text{g}/100\text{cm}^2$  (USEPA, 2008). However, these standards do not account for methamphetamine that diffuses into and is absorbed in the building surfaces, because “the extent to which meth and other lab-related chemicals migrate through materials and potentially volatilize is still unknown.” (USEPA, 2008). At present, there are no clean-up standards for methamphetamine concentrations in air. This may be due to a common assumption that methamphetamine is insufficiently volatile to pose a risk, other than through inhalation of contaminated dust. However, since the vapor pressure of free-base methamphetamine is equivalent to ~500 ppmv, even a small fraction of the vapor pressure can result in inhalation doses that rapidly surpass the recommended RfD (see section 1.2).

### **1.8. PERSISTENCE OF METHAMPHETAMINE IN LATEX PAINTED DRYWALL**

The Minnesota Pollution Control Agency performed wall board layering studies with methamphetamine in 2004. They found that for unpainted wallboard, which consists of gypsum held between a layer of front and back paper, most of the methamphetamine ended up accumulating in paper and not in the gypsum. Latex paint accounts for a large fraction of the surface area in an indoor environment (Sparks LE, et al., 1999). When latex painted wallboard was exposed to methamphetamine, most of the chemical showed up in the surface paint and not in gypsum (MPCA, 2004). Similar results were obtained when methamphetamine aerosolization was performed in a chamber installed with latex painted wall board (Martyny JW, et al., 2008). Depending on the recovery method, 35 – 85% of methamphetamine was recoverable from the surface. The remaining methamphetamine accumulated in the paint, not in gypsum (Martyny JW, et al., 2008). Encapsulating paint and oil based paint effectively reduced penetration of methamphetamine to the surface (Martyny JW, et al., 2008). However, approximately 20% of methamphetamine was able to penetrate a coating of latex paint (Martyny JW, et al., 2008). The reason may be attributed to the solubility of methamphetamine in water based latex paint relative to oil- based paint (Martyny JW, et al., 2008). Cooking methamphetamine results in two chemical forms which have different chemical and physical properties (MPCA, St Peter location, 2007). Methamphetamine

hydrochloride, which is a salt, does not directly volatilize under normal conditions; instead, it collects on surfaces and in dust (MPCA, St Peter location, 2007).

Methamphetamine, an intermediate base, is a vapor and can readily spread throughout the building structure (MPCA, St Peter location, 2007) and diffuse into and through building materials. Thus, even if the hydrochloride has been removed through vacuuming and washing surfaces, much methamphetamine can remain in the building structure.

### **1.9. MECHANISMS OF ACCUMULATION AND TRANSPORT OF ORGANIC COMPOUNDS IN BUILDING MATERIALS**

Indoor gaseous contaminants interact with the building materials by deposition from air onto the material surface and by adsorption/desorption. Sorption dynamics have been observed for walls and furnishings in a number of studies (Blondeau P. et al., 2008) (Tichenor et al., 1991, 1993) (Singer et al., 2007). Diffusion into and through materials can also occur; models that include diffusion coefficients and partition coefficients have been used to predict the accumulation and transport of organic chemicals in building materials (Little J et al., 1996) (ASHRAE 2001) (Haghighat F et al., 2002) (Meninghaus et al., 2002). Fickian diffusion has been observed for VOCs at concentrations typical of indoor environments (Little J et al., 1996) (Meninghaus et al., 2002). For transport that is not limited by gas-phase boundary layer phenomena, the partition coefficient and the diffusion coefficient are the most important parameters for most of the proposed VOC sorption models (ASHRAE 2001). The diffusion controlled sink model developed by Little et al., (1996), incorporates both parameters to predict the gas phase concentrations of a chemical in contact with the building material. For steady-state transport conditions, it is possible to simplify models to a single “effective diffusion coefficient” parameter. The effective diffusivity combines partitioning, gaseous diffusion through pores and internal sorption phenomena into a single parameter. Throughout this thesis, the term “diffusion coefficient” is equivalent to “effective diffusion coefficient”. Given the limited information on methamphetamine interactions with building materials, this study focuses on measuring this effective diffusion coefficient for typical wall-board configurations. With this parameter, and separately measured sorption capacity for insulation, accumulation rates within wall cavities can be estimated.



Fick's first law of diffusion relates the flux of a diffusing species in one direction to the concentration gradient in that direction. The equation is as follows,

$$J = -D \frac{dc}{dx} \quad (1)$$

Where,

$J$  - Flux of the chemical across a slab of building material, mg/m<sup>2</sup> sec

$D$  - Diffusivity or diffusion coefficient m<sup>2</sup>/sec

$\frac{dc}{dx}$  - Concentration gradient

For a slab (Cartesian coordinates) at steady state, the diffusion coefficient is,

$$D = -J \frac{\Delta x}{\Delta c} \quad (2)$$

Where,

$\Delta x$  - Thickness of the slab (m)

$\Delta c$  - Difference in concentration from one side of the slab to the other

The concentration can be measured within the slab material or in the fluid surrounding the material, resulting in two different effective diffusion coefficients. For estimating accumulation, air concentrations and exposure in buildings, an effective diffusion coefficient based on the air concentration is most convenient.

In addition to flux through wallboard, this study also seeks to understand accumulation in insulation materials. In estimating the partition coefficient of a chemical to a building material, the linear isotherm model is generally applicable (Yang X et al., 2001). The equation is as follows,

$$C_{air} = K C_{material} \quad (3)$$

Where,

$C_{air}$  - Equilibrium gas phase concentration, mg/m<sup>3</sup>

$C_{material}$  - Equilibrium material phase concentration, mg/m<sup>3</sup>

$K$  - Equilibrium partition coefficient, mg/mg

At steady state and at low VOC gas phase concentrations, the concentration of the chemical in the surface of the building material (mg/m<sup>3</sup>) is proportional to the concentration in the gas phase (mg/m<sup>3</sup>) just above the material.

## 1.10. MEASUREMENT OF THE EFFECTIVE DIFFUSION COEFFICIENT AND PARTITION COEFFICIENT

**1.10.1. Measuring effective diffusion coefficient ( $D_e$ ).** The cup method for VOCs and water vapor applies the one dimensional form of Fick's law for determining diffusion coefficients in building materials (ASHRAE 1997) (Kirchner S et al., 1999) (Hansson and Stymne 2000) (Haghighat.F et al., 2002). In the cup method, a pure source (e.g. water) is placed inside a cup. A material sample is then sealed to the top of the cup (Kirchner S et al., 1999). The compound diffuses through the material into "clean" air and, over time, the total mass of the system decreases. The cup is weighed periodically to determine weight loss of the compound. The rate of change of mass (mg/sec) is related to flux and the diffusion coefficient by the following equation (Kirchner S et al., 1999):

$$D_e = \frac{m}{A} \times \frac{L}{C_{saturation}} \quad (4)$$

Where,

$D_e$  - Effective diffusion coefficient, m<sup>2</sup>/sec

$m/A$  - Mass flux in mg/m<sup>2</sup> sec,

$L$  - Cross sectional length of the material

$C_{saturation}$  - Saturation concentration of the chemical in mg/m<sup>3</sup>.

Steady state diffusion coefficients for ethyl acetate and n – octane in six different types of building materials were determined using this method (Kirchner S et al., 1999). The measured diffusion coefficients for n-octane with a molecular weight of 114 g/mol in gypsum board was  $8.4 \times 10^{-7}$  m<sup>2</sup>/sec and for ethylacetate with a molecular weight of 88

g/mol to be  $1.1 \times 10^{-7} \text{ m}^2/\text{sec}$  respectively. The diffusion coefficient and partition coefficient are material properties and they are constant at a particular temperature and relative humidity. In our case, a modified cup method was designed to measure the effective diffusion coefficient in painted and unpainted drywall. The equation is as follows,

$$D_e \left( \frac{\text{m}^2}{\text{sec}} \right) = \frac{\text{Flux} \left( \frac{\text{mg}}{\text{m}^2 \text{ sec}} \right) \times L, \text{m}}{(C_{\text{saturation}} - C_{\text{out}}), \text{mg}/\text{m}^3} \quad (5)$$

Where,

$D_e$  - Diffusion coefficient in  $\text{m}^2/\text{sec}$ ,

$L$  - Cross sectional length of the material sample, m.

In our case the saturation concentration ( $C_{\text{saturation}}$ ) and the concentration diffusing out ( $C_{\text{out}}$ ) if the building material is measured. The flux is calculated based on the mass rate emitted along with the cross-sectional area of the material. See section 3.2.2 for details.

**1.10.2. Measuring partition coefficient (K).** A high resolution dynamic microbalance (0.1 – 0.5  $\mu\text{g}$ ) method (Cox SS et al, .2001) has been used to measure the equilibrium partition coefficient (K), for vinyl flooring (VF) for seven common types of VOCs, ranging in molecular weight of n-butanol to n-pentadecane also including water, phenol and toluene (Cox SS et al, .2001). The VF sample was placed in a microbalance, inside a chamber and a known concentration of VOC is passed into the chamber accounted as the sorption process. Weight gain of the sample is monitored until equilibrium is achieved. Equilibrium was assumed when the five point moving average of the mass change rate in the sample was 1% of the maximum rate of change. Since the difference in weight gain or loss (mg), the volume of the material ( $\text{m}^3$ ), the emission rate of chemical (mg/s) and the flow rate over the material ( $\text{m}^3/\text{s}$ ) are known, K can be calculated. A similar gravimetric procedure was followed in measuring the partition coefficient of NIBA sorbing to different kinds of insulation materials. See details in section 3.2.3

### 1.11. BOX MODEL TO PREDICT INDOOR METHAMPHETAMINE CONCENTRATION

The rate of change of contaminant concentration inside a building can be modeled using a box model, assuming the building is well mixed (Nazaroff and Case 1986). For steady-state systems, the indoor concentration ( $C_{air}$ ) is equal to the source rates (in mass rate units, e.g. mg/hr) divided by sink rates (in volumetric rate units, e.g.  $m^3 h^{-1}$ ). Sources can be direct emissions into the house, such as formaldehyde emitted from furnishings, mass delivered to the house by ventilation of contaminated outdoor air, or even the result of chemistry. Examples of sinks are ventilation (typically the most important removal mechanism), deposition to surfaces and chemical transformations.

$$C_{air} = \frac{\text{Source rates}}{\text{Sink rates}} \quad (6)$$

The concentration of airborne methamphetamine in a post-remediation house can be estimated using the same approach but may be the result of time dependent emissions. Figure 1.5 is a diagram of the simplified building model with a methamphetamine source and sink used to estimate the concentration of methamphetamine indoors. A mass balance on the methamphetamine concentration inside the house is given by the equation below.

$$V \frac{d C_{air}}{dt} = E(t) - Q C_{air} \quad (7)$$

Where,

$E(t)$  - time-dependent emission rate from contaminated surfaces, mg/sec

$V$  - volume of the house,  $m^3$

$Q$  - ventilation rate,  $m^3/s$

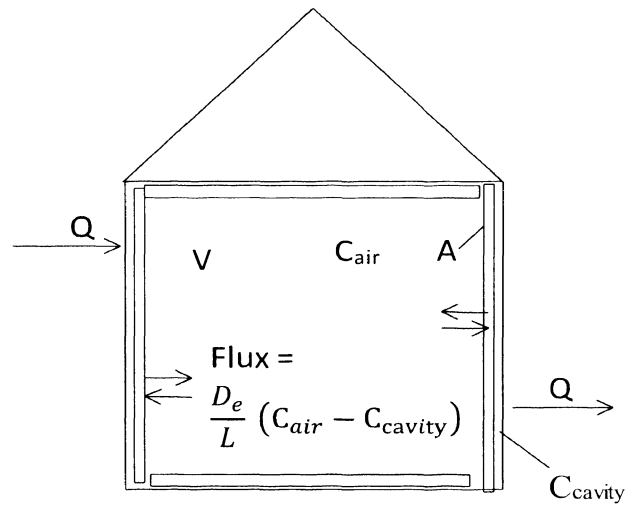


Figure 1.5. Box model to estimate the concentration of methamphetamine in a well-mixed house

Since methamphetamine is being emitted from an area source (walls, for this thesis), the emission rate,  $E(t)$ , is the contaminated wall area multiplied by the flux.

The emission rate from the wall cavity is,

$$E(t) = A \frac{D_e}{L} (C_{cavity}(t) - C_{air}) \quad (8)$$

Where,

$C_{cavity}$  - concentration of methamphetamine in the wall cavity air,  $\text{mg}/\text{m}^3$

$D_e$  - effective diffusion coefficient ( $\text{m}^2/\text{s}$ )

$L$  - wall thickness (m)

$A$  - total wall area subject to accumulation,  $\text{m}^2$

The flux of methamphetamine through a wall is assumed to follow Fick's first law, where steady-state flux is proportional to the diffusion coefficient and the concentration gradient across the gypsum drywall. The concentration difference between the wall cavity and the room drive the emissions into the room. The accumulation phase, during a meth cook, is modeled using a similar approach but includes accumulation in wall-cavity insulation. The development and solution of the accumulation phase and release phase models are described in section 3. and the results are discussed in section 4.

#### **1.12. WALL ASSEMBLY OF A BUILDING AND METHAMPHETAMINE CONTAMINATION**

According to a housing survey conducted by the U.S.Census in 2009, the median age of all homes in US is around 36 years and 22% of the houses in US were built during 1950's and 1960's. The inclusion of a vapor retarder in a wall assembly commenced in 1920's (United States Department of Housing and Urban Development, 1999 [USDHU]).

The wall assembly of a residence typically has the following components in its cross section. It includes, latex painted gypsum board on the side facing the indoor environment, a vapor barrier, cavity insulation with concrete block, drained cavity and brick/stone veneer or wall board on the exterior ( Listiburek, 2006). Vapor barriers are installed to prevent the entry of water vapor to the interior (Listiburek, 2004). This eliminates condensation of water in between the structural components and prevents mold growth (Listiburek, 2004). The components in the cross section, especially the vapor barrier can be installed either towards or away from the indoor environment. This is important because vapor barriers immediately behind the wall board or in front of the insulation could prevent methamphetamine accumulation in insulation. Vapor barriers behind insulation would promote accumulation in the wall cavity by preventing transport to outdoor air. Poorly installed vapor barriers, even on the inner side of the cavity, may not pose a significant barrier to methamphetamine accumulation in the cavity and in insulation. Different combinations of wall assemblies are available and the types that might result in contamination behind the wall surface are as follows (Listiburek, 2004),

- a) Frame wall with exterior insulation and brick or stone veneer
- b) Frame wall with cavity insulation and brick or stone veneer

- c) Concrete block with interior frame wall cavity insulation and brick or stone veneer

Each of these combinations has the vapor barrier on the outer side of the wall cavity thus exposing the insulation for contamination. Figure 1.6 shows these combinations of wall assembly components.

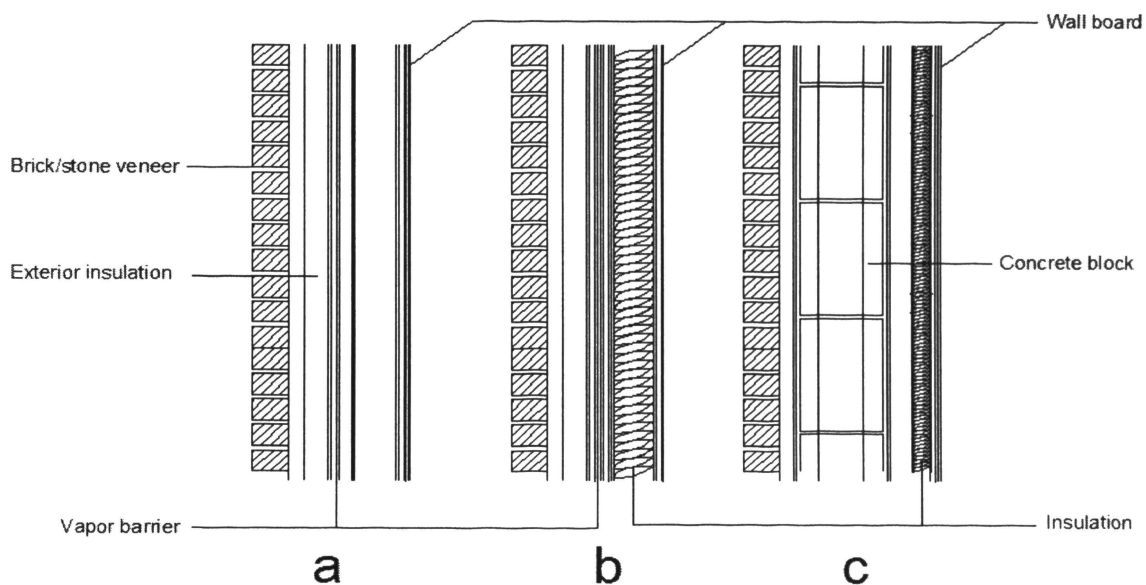


Figure 1.6. Three different types of wall assemblies with vapor barrier on the exterior side

### 1.13. PURPOSE OF RESEARCH

This research is a part of a larger research project initiated by Missouri University of Science and Technology, National Institute of Standards and Technology and University of Texas, Austin. The overall objective was to estimate indoor air concentrations of methamphetamine (and occupant exposure) due to re-emission of methamphetamine from building materials into the indoor environment. Other parts of the project have

measured and modeled methamphetamine sorption and re-emission from painted surfaces. This research focuses on flux through drywall into insulation and subsequent re-emission. The diffusion coefficient of methamphetamine in drywall and painted drywall is measured to quantify the diffusive resistance offered by these materials. Also, the partition coefficient for two types of insulation, cellulose and fiber glass is measured. These measurements are incorporated into a model of accumulation and release intended to estimate indoor concentrations (and occupant dose) of methamphetamine during post-remediation occupation. The dose is compared to a reference dose to estimate the time required for the indoor concentrations to become acceptable.



## **2. GOALS AND OBJECTIVES**

Cooking methamphetamine indoors generates methamphetamine vapor that penetrates painted surfaces and results in (potential) contamination of insulation, vapor barriers and wood studs. Clean-up guidelines for methamphetamine allow for washing surfaces to remove surface contamination. Methamphetamine that has penetrated into building materials can be re-emitted, exposing future occupants to unacceptably high concentrations. Thus the goal of this research is to determine if building materials like cavity insulation can act as a significant reservoir for methamphetamine and significantly elevate the concentration during post-clean-up occupancy. To achieve this goal the following objectives were established,

### **2.1. OBJECTIVE 1: MEASURE THE EFFECTIVE DIFFUSION COEFFICIENT OF PAINTED DRYWALL**

Methamphetamine has been found to diffuse into paint; drywall is very porous but does not seem to be a significant accumulator. To understand the potential sink and source effect of building walls, the effective diffusion coefficient of plain drywall and painted drywall were measured using a modified cup/flow-through chamber method. Using the effective diffusion coefficient the resistance to diffusion offered by painted drywall can be estimated.

*Hypothesis:* Drywall is anticipated to pose a modest resistance to diffusion of methamphetamine, but latex paint is expected to accumulate methamphetamine and thereby offer greater resistance to diffusion.

### **2.2. OBJECTIVE 2: MEASURE THE PARTITION COEFFICIENT OF METHAMPHETAMINE IN INSULATION**

For walls that do not have a vapor barrier on the interior side of the wall cavity, methamphetamine can be sorbed by insulation materials in outer walls. Thus, insulation can act as a significant sink and reservoir for methamphetamine.

To quantify the sink potential and to estimate the impact on indoor air quality, the equilibrium partition coefficient of two types of typical wall insulation was measured.

*Hypothesis:* The partition coefficient of cellulose insulation is expected to be larger than fiber glass.

### **2.3. OBJECTIVE 3: ESTIMATE THE ACCUMULATION AND THE RESULTING METHAMPHETAMINE AIR CONCENTRATION DUE TO REEMISSION**

During the cooking process, methamphetamine vapors can diffuse through the painted drywall assembly and accumulate in the insulation of a residence. Then the methamphetamine can be reemitted into the building, resulting in exposure to future occupants. The accumulation phase and reemission phase are modeled to estimate occupant exposure.

*Hypothesis:* The dynamic post-remediation indoor concentration strongly depends on permeability of drywall and the type of insulation in wall cavities.

### **2.4. OBJECTIVE 4: ESTIMATE THE ACCUMULATED METHAMPHETAMINE DOSE FOR ADULTS AND CHILDREN AND THE TIME REQUIRED TO REACH A SAFE INDOOR CONCENTRATION**

Due to the dynamics of methamphetamine accumulation and decay, the post-remediation occupants may inhale higher than recommended doses of methamphetamine. The chronic daily dose of methamphetamine is estimated using an intake equation developed by the US EPA to assess health risk (Murnyak G, et al., 2011).

*Hypothesis:* Post-remediation occupants are subject to an inhalation dose that is several orders of magnitude greater than the sub chronic reference dose soon after re-occupation. The time required to reach safe concentrations, or safe daily dose, indoors is greater than one month.

### 3. MATERIALS AND METHODS

#### 3.1. MATERIALS

**3.1.1. Building materials.** Drywall and painted drywall were used for determining the effective diffusion coefficient of NIBA and water. Each sample has a circular geometry, 15 cm in diameter. The outer edge is sealed with aluminum foil tape, wrapped to about 2cm from the edge. The circular samples are sealed to a pyrex cup (described below) and the foil tape is applied so that no NIBA or water leaks from outer edge of the sample. The actual area for flux is  $0.018\text{m}^2$ . Two types of plain drywall U1 and U3 and latex painted drywall P1 and P2 were used for the diffusion experiments. The drywall are Sheet Rock brand, manufactured by United States Gypsum. The two types of paint on the drywall include, 100% acrylic, flat finish(light blue) paint from Benjamin Moore and, white satin latex paint P2 from Sherwin Williams. The painted drywall was allowed to dry/cure in the laboratory for several years before use.

**3.1.2. N- isopropylbenzylamine.** Research grade, 97% pure liquid, product number 136964, purchased from Sigma Aldrich was used for the gas phase standard and diffusion experiments.

**3.1.3. Toluene.** Spectro grade, 99.5% pure liquid, product number 42117 – 5000, purchased from ACROS was used to spike the toluene concentration during GC analysis to find the concentration of toluene (a contaminant) in gas phase NIBA samples.

**3.1.4. Insulation.** Blown in natural fiber (R13-R60) from green fiber and glass fiber (R-13 and R-30) cavity insulation from Johns Manville, item No B-1284 & B-390 were chosen to measure the partition coefficient of NIBA at  $25^{\circ}\text{C}$ .

**3.1.5. SPME fibers.** The SPME fiber is assembled into a manual holder with a spring. The holder is made of metal alloy and has a 24 gauge needle. The fiber is a Stable Flex SS, pink/plain,  $65\ \mu\text{m}$  coated with polydimethylsiloxane/divinylbenzene (PDMS/DVB).

**3.1.6. HOBO data logger.** The U12 Temperature/relative humidity/2 external channel data logger was used to measure the water concentration while measuring water diffusivity for samples U3 and P2.

## 3.2. EXPERIMENTAL METHODS

**3.2.1. Objective 1.** To meet objective 1, the flux through drywall samples is measured and, using equation 5, the diffusion coefficient is calculated. Section 3.2.1.1 describes the experimental apparatus used to measure the flux. Briefly, humidified air flows into a chamber containing the drywall sample held sealed to the cup containing a pure chemical. The chamber is well mixed and the outlet concentration ( $C_{out}$ , resulting from diffusive flux through the drywall) is measured using a solid phase micro extraction (SPME) fiber in a dynamic sampler. To calibrate for a wide range of conditions, two separate gas calibration systems, a low range concentration ( $\sim 80$  ppb) and, high range concentration ( $\sim 400$  ppb) were developed. The gas concentration in the cup ( $C_s$ , below the drywall sample) is measured using a static, time-averaged, SPME technique. Section 3.2.1.2 and section 3.2.1.3 describes analytical methods used to calibrate the SPME in the dynamic sampler. Section 3.2.1.5 describes the apparatus used to measure the vapor pressure of pure NIBA. Section 3.2.1.5.3 describes methods for measuring the saturation concentration of NIBA over the pure material obtained from Sigma-Aldrich. Section 3.2.1.6 describes static SPME method used to measure the concentration inside the cup (below the sample). Note that the diffusivity of water was also measured using similar procedures.

**3.2.1.1 Apparatus and procedure used for determining the diffusion coefficient for building material.** The apparatus shown below in Figure 3.1 was used to measure the steady state diffusion coefficient of gas phase NIBA diffusing out of drywall and painted drywall.

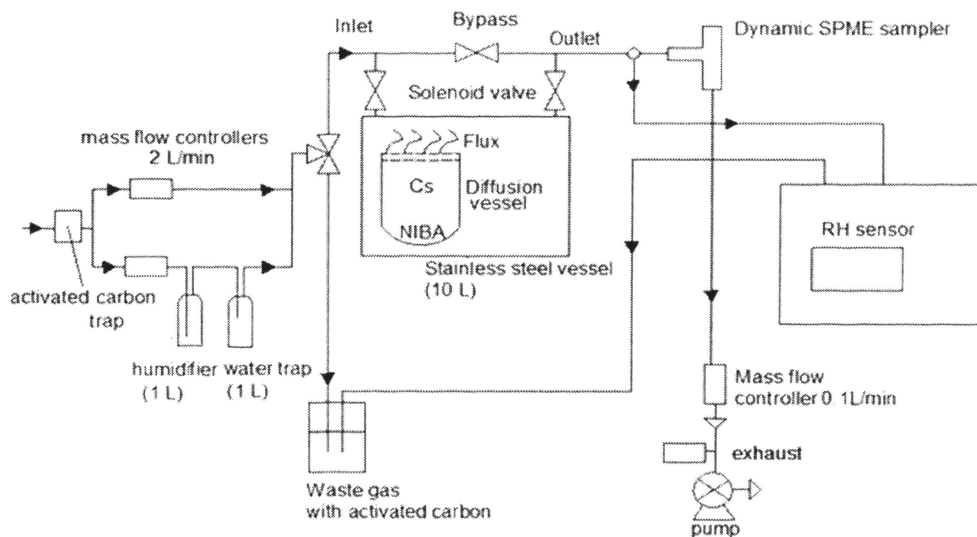
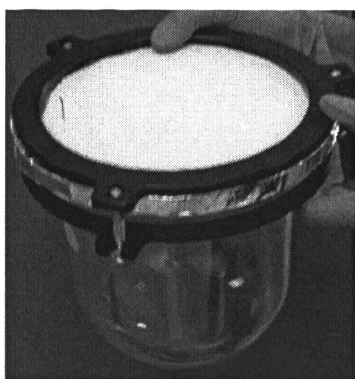


Figure 3.1. Apparatus showing diffusion setup

**3.2.1.1.1 Diffusion vessel/reaction flask.** The diffusion setup is a reaction flask made of pyrex glass with a capacity of 2000 mL. Figure 3.2a & 3.2b shows the actual diffusion flask and its accessories.



3.2a



3.2b

Figure 3.2a & 3.2b. Shows the drywall and glass pyrex diffusion flask

The upper portion of the reaction flask is provided with an O-ring flange which is 168 mm in diameter. The flange is provided with three copper screws which can be screw tightened so that the drywall is held in between the flange at top portion of the reaction flask. About 2 ml of pure NIBA liquid (or solution) is introduced into the vessel before the experiment. The drywall sample then is sealed with the back (unpainted) facing down towards the cup. The side that is normally painted is facing upward, in contact with the diluent air in the outer chamber. The reaction flask is then placed inside a stainless steel vessel.

**3.2.1.1.2 Outer flow-through chamber.** The outer chamber is a 10L stainless steel cylindrical container that was electro- polished by the manufacturer (Eagle stainless). Two ports ¼” ports (inlet and outlet) are located on top of the lid to allow air to access the chamber. The air is purified using an oil trap and an activated carbon trap (organic vapor specific). The flow rate of air is controlled by two mass flow controllers; one is passed through a water bubbler to humidify the air. In combination, the two streams are combined for a total flow rate of 2L/min and 50% relative humidity. NIBA diffusing out was sampled and the valve timing was all controlled by an in-house data acquisition system (Lab view). The entire system was set inside a walk – in temperature controlled chamber operated at 25°C for the entire experimental period.

**3.2.1.1.3 Sampling procedure and steady state concentration  $C_{out}$ .** Samples are collected by exposing the SPME fiber for 5 minutes and analysed using the GC/MS to check for background before introducing the chemical. After the chemical is introduced beneath the sample in the diffusion flask, a 5 min sample for response is performed to check for any leaks in the system. A large peak of NIBA observed in the first few hours indicates a leak in the diffusion setup. Five minutes is chosen as default sampling time based on calibration studies. The chemical then reaches a steady state concentration. The resulting value of  $C_{out}$  is used in calculating the diffusion coefficient.

**3.2.1.1.4 Equations to calculate  $D_e$ .** The equation used to calculate the steady state flux and effective diffusion coefficient is as follows,

$$\text{Steady State flux, mg/m}^2\text{hr} = \frac{C_{out, \mu\text{g/m}^3} \times \text{Flow rate, Q, m}^3\text{/sec}}{\text{Area, A, m}^2} \quad (9)$$

$$\text{Effective diffusion coefficient } D_e = \frac{\text{Flux} \times L}{(C_s - C_{out})} \quad (10)$$

**3.2.1.2 Apparatus used to generate a low concentration (ppb) standard for the diffusion experiment.** The apparatus shown in Figure 3.3 was used to calibrate the SPME fiber for low-concentration (~ 80 ppb) dynamic sampling.

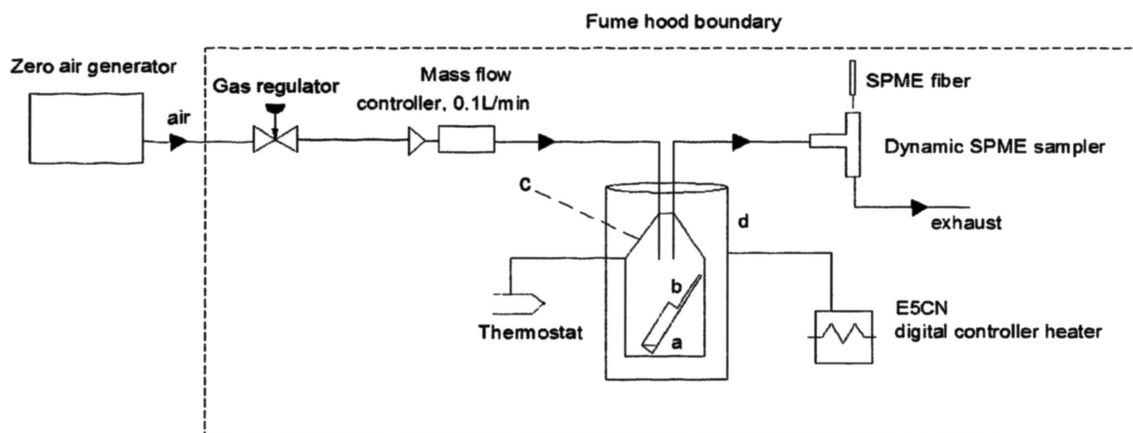


Figure 3.3. Experimental apparatus for low range calibration.

97% pure NIBA (~1 ml) is introduced into a diffusion vial (a). The diffusion vial is made of glass, with a capillary stem (b) above the main body of the vial with a length of 7.5 cm and capillary diameter of 0.2 cm. The diffusion vial is placed inside a glass bottle (c) with a capacity of about 2 L. The initial mass of the vial ( $W_0$ ) without NIBA is measured before introducing NIBA into the glass bottle so that the mass of pure NIBA ( $W_1$ ) in the vial can be weighed gravimetrically at time  $T_1$ . The bottle is placed inside a hollow

cylindrical heater (d) made of aluminum. The glass bottle is slid into the heater so that the walls of the bottle are in contact with the walls of the heater. The aluminum cylinder is heated with the help of a digital controller set at constant temperature of 35°C. Pure air is introduced into the glass bottle with the help of a 2 L/min mass flow controller for the flow rate to remain stable over a long period. The flow out of the bottle is sampled with the help of a 3/8 inch (95 mm) stainless steel compression tee (Swagelok, Solon, OH) used as the main body of a dynamic SPME sampling device (S. Shu. et al., 2010). A modified Teflon Mininert valve body (Supelco, Bellefonte, PA) with a septum seal was inserted into the tee to center and stabilize the SPME needle. The flow rate through the dynamic sampler was controlled at 0.1 L/min. The flowing gas mixture is sampled by exposing the fiber at different time intervals. Exposing the fiber to a regulated flowing stream reduces the boundary layer resistance to mass transfer and improves reproducibility. For short sampling times (< 20 minutes) the mass rate of accumulation on the fiber is linearly related to sampling time, indicating that this is in the transport limited regime; this also helps promote reproducible sampling and reduces uncertainty due to temperature variations. The mass of the vial ( $W_2$ ) after a certain time period  $T_2$  is measured. From the flow rate (L/min) and from the difference in weight of NIBA ( $W - W_2$ , grams) at known time interval ( $T_2 - T_1$ ) (min), the emission rate (g/min) of NIBA from the diffusion vial is calculated. The equations used to quantify the emission rate and resulting concentration of NIBA is shown below,

$$\text{Mass of NIBA } W, g = (W_0 - W_1) \quad (11)$$

$$\text{Emission rate } E, \frac{g}{min} = \frac{(W - W_2)g}{(T_1 - T_2) min} \quad (12)$$

$$\text{Concentration out, } \frac{g}{L} \text{ or } \frac{\mu g}{m^3} = \frac{E, g/min}{Flow rate, L/min} \quad (13)$$

$$\text{Mixing ratio, ppb} = \left( \frac{\mu g}{m^3} \right) \times \frac{24.45}{molecular weight} \text{ at } 25^\circ C \quad (14)$$



**3.2.1.2.1 SPME/GC/MS.** Each SPME sample was analyzed immediately after sample collection. An Agilent gas chromatograph mass selective detector was used in analyzing the SPME sample. A 65 $\mu\text{m}$ , PDMS/DVB, stable flex/SS SPME fiber was used to sample. A liner with a 0.75mm inner diameter was used in the injection port. The injection port was maintained at 260°C for fast desorption at a split ratio of 10:1. The SPME fiber was retained in the injection port for 5 minutes. A single fiber was repeatedly used in all the experiments. An HP – 5MS, (30.0 m x 250 $\mu\text{m}$  x 0.25  $\mu\text{m}$ ) capillary column was used under 6.40 psi constant pressures. The oven temperature ramp was 100°C to 280°C at a rate of 20°C/min. MS detector port was set at 260°C. The total run time was 9 minutes.

**3.2.1.2.2 Calibration procedure.** The SPME fiber was exposed in the dynamic sampler (section 3.2.1.1.3) to a gas concentration of 80 ppb. Sampling times of 30sec, 1min, 3min and 5 min were chosen to check for the linear response using SPME fiber. A sampling time of 5 min was chosen for sampling  $C_{out}$  in chamber experiments based on results of calibrations.

**3.2.1.3 Apparatus used as a high concentration (ppm) standard for diffusion experiment.** The apparatus shown in Figure 3.4 was used to measure gas phase, high concentration (~ 400 ppb) NIBA diffusing out of a diffusion vial.

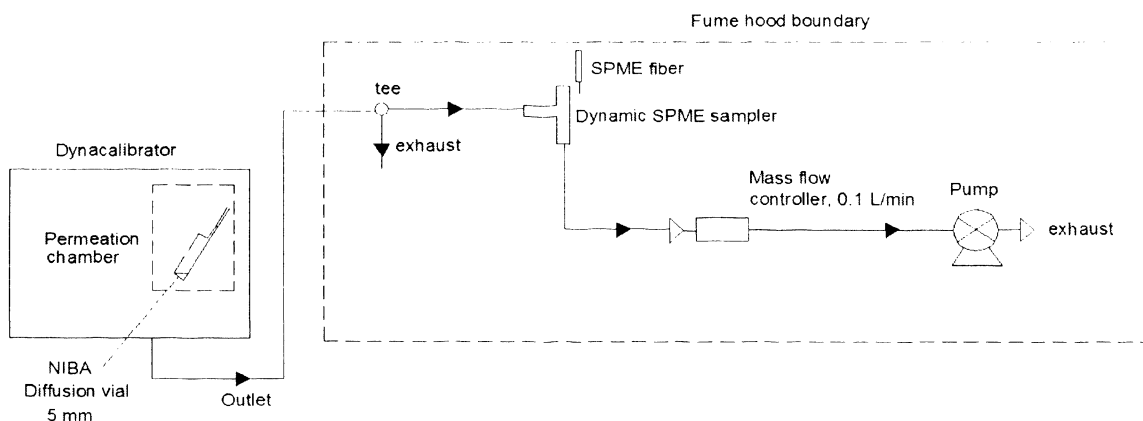


Figure 3.4. Experimental setup for high range calibration

A VICI Metronics Dynacalibrator, model number 230, was used to generate a constant gas mixing ratio of NIBA. The instrument can generate parts per million ranges or lower for both organic and inorganic compounds. A diffusion vial as described in the previous section with a capillary diameter of 0.5 cm is placed inside a permeation chamber of the system. This chamber receives a fixed flow carrier gas stream of pure air, which controls the permeation rate of a calibration gas, in this case pure NIBA inside the diffusion vial. The carrier gas stream flows through the permeation chamber, mixes with the calibration gas at the mixing tee. The chamber temperature is maintained at 35 °C. The differential pressure regulator and carrier flow restrictor before the permeation chamber provide a stable carrier flow rate to the chamber. The flow rate of carrier flow is set at 0.165 L/min. The outlet from VICI system is connected to dynamic SPME sampler as described above. A portion of calibration gas from the tee (0.1 L/min) is drawn into the dynamic sampler using a 0.2 L/min mass flow controller and a pump. As described above the mass of the diffusion vial is measured periodically to determine the emission rate of NIBA from the vial. With respect to sampling and chemical analysis, the same procedure is followed as described in section 3.2.1.2.1.

**3.2.1.3.1 Calibration procedure.** The SPME fiber was exposed in the dynamic sampler (section 3.2.1.1.3) to a gas concentration of about 400 ppb. Sampling times of 30sec, 1min, 3min and 5 min were chosen to check for the linear response using SPME fiber. A sampling time of 5 min was chosen for sampling  $C_{out}$  in chamber experiments based on results of calibrations.

**3.2.1.4 Measuring the diffusion coefficient of water in samples U3 and P2.** To validate the cup method for measuring effective diffusivity, the diffusion coefficient of water was measured and compared against published values. The same apparatus as described in section 3.2.1.1 is used. The cup is filled with Milli-Q water and the outlet from the flow through chamber is passed into a second 10L stainless steel chamber. In this chamber, a HOBO humidity transducer is used to measure the relative humidity of the outlet air due to water that has diffused through the drywall.

**3.2.1.4.1 Procedure for calculating diffusion coefficient using water vapor permeability values in gypsum board and painted gypsum boards.**

The steady state flux due to water diffusing out of the drywall samples can be equated using two different material properties ( permeability,  $\tau_p$ , and diffusion coefficient,  $D_e$ ).

The permeability is calculated as follows,

$$\tau_p = \left( \frac{M \times L}{A \times \Delta t \times \Delta p} \right) \quad (15)$$

Where,

$\tau_p$  - water vapor permibailty values, g /m s pa

$M$  - Mass of water that has transported through the material over time interval  $\Delta t$ , g

$L$  - thickness of the material, m

$A$  - exposed surface area, m<sup>2</sup>

$\Delta t$  - time interval, sec

$\Delta p$  - pressure difference, pa<sup>-1</sup>

Since,

$$Flux_{steady\ state} = \left( \frac{M}{A \times \Delta t} \right) \quad (16)$$

Combining equations 15 and 16,

$$Flux_{\ steady\ state} = \left( \frac{\tau_p}{L} \Delta p \right) \quad (17)$$

Combining equation 5 from section 1.10.1 with equations 16 and 17,

$$\left( \frac{\tau_p}{L} \Delta p \right) = D \times \frac{(AC)}{L} \quad (18)$$

Using the ideal gas law,

$$\tau_p \times \Delta p = D \times \frac{(MW)}{R T} \Delta p \quad (19)$$

Therefore,

$$\tau_p = D \times \frac{(MW)}{R T} \quad (20)$$

Thus the predicted  $C_{out,water}$  from the literature is used to calculated using the equation below,

$$C_{out,water} = \left( \frac{ip \times R \times T}{MW} \right) \times (Cw, sat) \times \left( \frac{A}{Q \times L} \right) \quad (21)$$

The predicted  $C_{out,water}$  is used in equation 5 to estimate the effective diffusion coefficient due to water and will be compared against measurements made in this research.

**3.2.1.5 Apparatus used for measuring vapor pressure of NIBA.** The apparatus shown below is a saturator, used for measuring vapor pressure of pure NIBA.

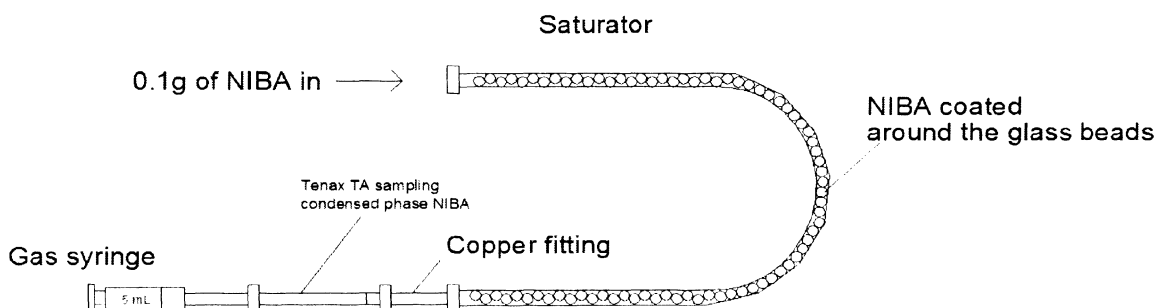


Figure 3.5. Saturator – Tenax TA apparatus for measuring vapor pressure

The saturator is a teflon tube of length 1m, with an inside diameter of 2 mm, filled with 1mm glass beads. The glass beads are relatively large so as to limit pressure drop (Bruno TJ et.,al 2010) and so that they do not significantly impede the flow of gas through the saturator. Although they are large, they provide sufficient surface area to allow gas passing through the device to become saturated as it contacts the beads which are coated with the low-volatility chemical (Bruno TJ et.,al 2010). One advantage of using a saturator such as this is that the amount of chemical needed to saturate the gas stream is very much reduced (Bruno TJ et.,al 2010). For this experiment a 10% (v/v) solution of NIBA in acetone was used to coat the internal surface of the saturator. Approximately 1mL (0.1 g) of the solution was used to wet the saturator internal surface. After wetting the surfaces, clean dry air was passed through the saturator at 0.1 ml/min for 30 minutes

to evaporate the acetone, leaving the beads coated uniformly with NIBA. Standard compression fittings are used to seal the ends of the tube and also enable the TENAX tubes to be inserted at the ends. One end of the TENAX tube is fitted to the Teflon tube and the other end is fitted to a 50 ml syringe (Warner instruments). As the sample is drawn through the Teflon tube fitting, the opposite fitting of the saturator is loosened to enable air flow to flow through the saturator. The whole apparatus is housed in a temperature controlled chamber maintained at 25°C. To quantify the mass accumulated in the TENAX from saturator, replicate samples of known concentration (~ 400 ppb) from the dyna calibrator system is used as a standard.

**3.2.1.5.1 TENAX/FID.** The mass accumulated on a TENAX tube is analyzed using a GC/FID – (gas-chromatograph/flame ionization detector), with the help of a thermal desorber and auto sampler connected to it. An Agilent gas chromatograph flame ionization detector (GC/ FID) was used in analyzing the TENAX sample. The injection port is connected to the thermal desorber which injects the sample into the back inlet of the system. The injection port was maintained at 260°C for fast desorption at split less mode. After the initial desorption for 10 min, the injection is done based on the sequence generated in the GC. A HP – 5, 5% Phenyl Methyl Siloxane, 30m x 320µm x 0.25µm, and capillary column were used under constant pressure. The oven temperature ramp was 100°C to 280°C at a rate of 20°C/min. FID detector port was set at °C. The total run time was 14 minutes.

**3.2.1.5.2 Sampling procedure and calibration.** The sampling procedure for the saturator involves sampling different volumes of gas onto TENAX tubes using a gas syringe. Sample volumes of 5, 10, 15, 20 and 30 ml were chosen to inject into the Tenax and analyse using the GC/FID. To calibrate the response from the saturator apparatus, a volume of a known chemical concentration from the Dynacalibrator was sampled for varying sampling times to obtain the mass response from the FID. The slopes of the responses were compared to obtain the measured vapor pressure using following equations.

$$C_{saturator} = \frac{\text{Slope saturator (Peak area/Volume)}}{\text{Slope dynacalibrator (Peak area/Volume)}} \quad (22)$$

$$\text{Vapor pressure, } PV_{STP} = \frac{C_{\text{saturator}}}{MW} \times 10^6 \times RT \quad (23)$$

**3.2.1.5.3 SPME calibration for pure NIBA.** The concentration of NIBA below the drywall sample (Figure 3.6) is quantified in this research using a static SPME measurement (described in more detail in section 3.2.1.6). The rate of mass accumulation in a static system is lower than for the flowing sampler described in section 3.2.1.2. To calibrate the static sampling system, the SMPE fiber was exposed to NIBA gas at equilibrium with a pure NIBA liquid sample in a 1 ml bottle. A 30 sec sample was found to provide an adequate and reproducible signal. This signal was considered proportional to the saturation concentration measured using the saturator.

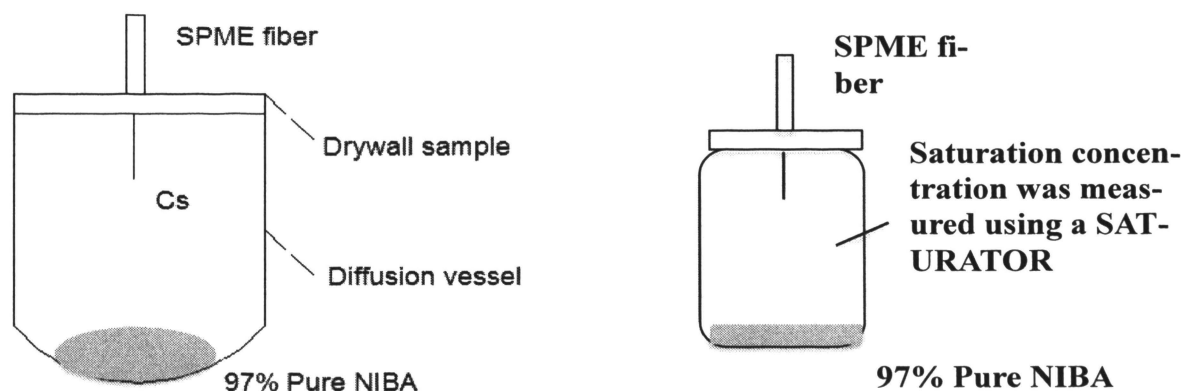


Figure 3.6. Measuring concentration beneath the drywall sample

**3.2.1.5.4 SPME/GC/MS.** Each SPME sample was analyzed immediately (within 5 minutes) after sample collection. The analytical instrument used to analyse the sample is the same as described in section 3.2.1.2.1 Since the sample is a static pure NIBA sample, a split ratio of 140:1 was required to prevent saturation of the GC/MS detector. The response for pure NIBA using SPME is listed in APPENDIX A.

**3.2.1.6 Measuring the saturation concentration beneath the sample in diffusion experiment.** Although the concentration below the sample is intended to be at saturation, low-volatility impurities in the NIBA sample can reduce the actual concentration below that measured for pure NIBA, especially after many days of NIBA evaporation. The concentration below the drywall sample is measured after the gas-phase SPME response is considered to be at steady-state (see section 3.2.1.2). To measure the concentration, a small drill is used to bore a 0.1mm diameter hole in the drywall sample. A stainless steel needle is inserted into the hole to stabilize the SPME needle as it is inserted through the drywall sample and exposed to the gas beneath the sample. A 30 sec sample is collected as described in section 3.2.1.5.4 and compared against the static signal for pure NIBA. Figure 3.7 shows the stainless steel needle, inserted through the drywall sample, ready to be sampled using SPME. The response for the below-drywall concentration for samples U1 and P1 are tabulated in the APPENDIX A.

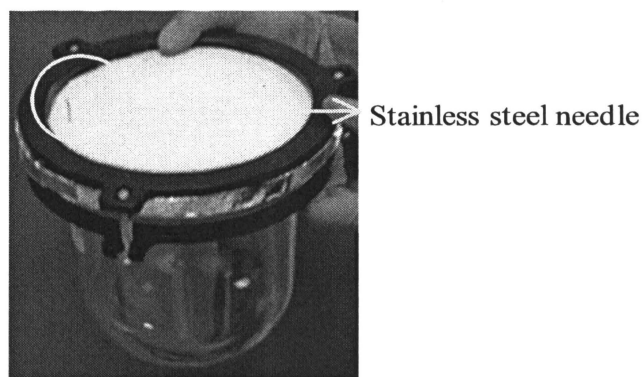


Figure 3.7. Showing the stainless steel needle inserted into the sample

### 3.2.1.7 Toluene contamination elimination

Early in the research NIBA from the manufacturer was observed to have toluene as a volatile contaminant. Toluene emitting from diffusion tubes would complicate

gravimetric calibrations. To eliminate the toluene emitting from the solution, air or nitrogen was bubbled into a solution (~1 gram) of pure NIBA contained in a glass bubbler at a flow rate of about 0.9 L/min. The apparatus was then weighed periodically until; there was a 20% reduction in the mass of NIBA inside the apparatus. The headspace of pure NIBA was then analyzed in the GC, using a SPME sampler to ensure the toluene was eliminated.

**3.2.2. Objective 2.** The equilibrium uptake of NIBA in insulation was measured by measuring the mass increase in the sample of insulation using a microbalance. The gas phase concentration inside a desiccator chamber,  $C_{\text{air}}$  is maintained at 10% of the vapor pressure of NIBA using a mixture of NIBA in polydimethylsiloxane (PDMS) oil. Based on the mass uptake of NIBA and the density and volume of the insulation, the concentration accumulated in the material  $C_{\text{material}}$  was calculated.

**3.2.2.1 Experimental procedure.** Metal weigh-boats were used to hold the insulation samples for this experiment. A Mettler – Toledo scale with sensitivity to 0.00001 g was used for gravimetric measurements. Two glass desiccators and two glass dishes, rinsed with methanol were used as the exposure chamber and reservoir for NIBA respectively. One of the glass dishes was filled with 10 mL of pure NIBA and placed in a desiccator, and the other glass dish was filled with a 10 mL mixture of 10% (1 mL) NIBA and 90% (9 mL) silicone oil and placed into the other desiccator. Empty weigh boats were measured and then the weight of the insulation alone was measured. Four of the boats were left empty as a control. These boats were placed on metal trays, and placed inside the desiccator. The whole setup was placed inside a walk in temperature controlled chamber at 25°C. Figure 3.8 shows the desiccator and the weighboats with the insulation samples. The insulation samples were weighed daily until there was less than 5% difference in mass between days. The uptake (g/g) of NIBA was obtained by dividing the change in mass over the weight of the insulation. The density was obtained by taking 3 samples of each type of insulation, weighing them, and determining the dimensions. R-13 and R-30 were cut into squares, and the length, width, and height of the squares were measured. The blown-in natural fiber was packed into a 300 mL beaker to simulate the packing in a wall cavity, and then weighed. All of the samples were weighed using a



Denver Instruments A-160 scale. The density was used to convert the mass uptake of NIBA for the respective insulations into a concentration ( $\text{g}/\text{m}^3$ ). The concentration of NIBA in the vapor phase was calculated by using the Ideal Gas Law ( $PV = nRT$ ). The vapor pressure at 10% concentration was assumed to be 10% of the total vapor pressure. The partitioning coefficients were found by dividing the concentration of NIBA in the insulation by the concentration in the vapor phase (see equation 3), and averaged over all samples for each type of insulation.

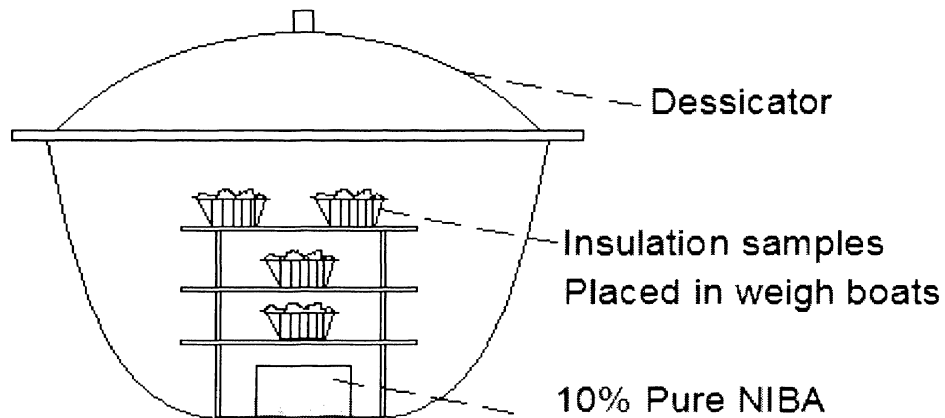


Figure 3.8. Measuring the weight gain in insulation

**3.2.3. Objective 3 and 4.** The accumulation of methamphetamine in insulation during a two week cooking process was modeled. Two main assumptions were that the bulk phase concentration of methamphetamine in air was at 0.1% of the published vapor pressure at  $25^{\circ}\text{C}$  and the flux through the wall was at a pseudo-steady state for short time intervals (but not over the long-term). A separate release phase was modeled to determine the concentration in room air  $C_{\text{air}}$  by performing a mass balance on the building and assuming rapid decay of  $C_{\text{air}}$  to pseudo-steady state relative to rapid changes due to air-exchange. The release phase model was used to predict the time dependent indoor air

concentration and, from this model, the time period required to reduce the concentration to a specified safe concentration was determined. A USEPA inhalation dose method was used to estimate the methamphetamine dose during the time interval when methamphetamine was above safe concentrations.

**3.2.3.1 Dynamic approach for accumulation of methamphetamine through drywall during a two week cooking process.**

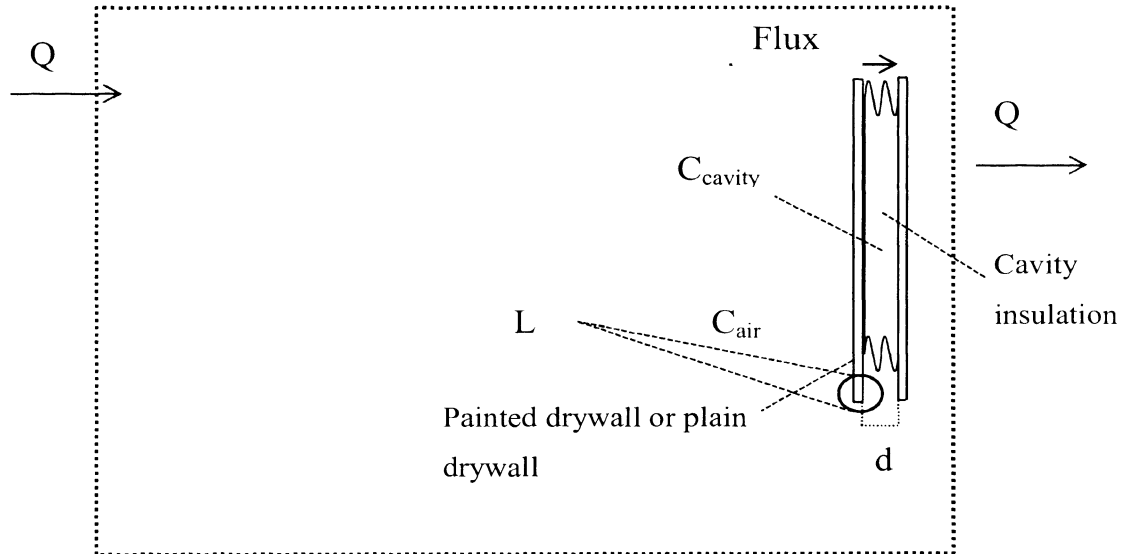


Figure 3.9. Accumulation and release of methamphetamine behind the wall assembly

**3.2.3.1.1 Phase 1: Accumulation**

Mass accumulation in the insulation of a wall assembly depends on mass transfer (diffusivity, concentration gradients) and equilibrium partitioning of methamphetamine to the insulation of a building (partition coefficient).

$$M_{cavity} = C_{cavity} \times \epsilon_b \times V + C_{cavity} \times K \times \rho \times V$$

During the two week cooking process, the flux into the insulation brings about a dynamic change in the concentration of methamphetamine in the wall cavity.

flux  $\times$  area = mass accumulation rate in cavity. Assuming Fick's first law holds, the flux is proportional to the concentration difference across the drywall, the diffusion coefficient and the reciprocal of the drywall thickness:

$$\frac{dM_{cavity}}{dt} = \frac{D_e}{L} (C_{air} - C_{cavity}) \times A$$

Mass accumulation for the required surface area and volume of insulation due to methamphetamine flux into the insulation and partitioning to the insulation is given by,

$$\frac{D_e}{L} (C_{air} - C_{cavity}) A = \frac{d(C_{cavity} \times \epsilon_b \times V + C_{cavity} \times K \times \rho \times V)}{dt}$$

Where,

$\epsilon_b$  - porosity of insulation, assumed to be 0.95

$V$  - Volume of the house, m<sup>3</sup>

$\rho$  - Density of insulation, mg/m<sup>3</sup>

$$\frac{D_e}{L} (C_{air} - C_{cavity}) A = \frac{d(C_{cavity})}{dt} V (\epsilon_b + K')$$

Replacing,  $V = A \times d$

Where,

$d$  - thickness of insulation, m

$$\frac{d(C_{cavity})}{dt} = \frac{D_e (C_{air} - C_{cavity})}{L (\epsilon_b + K') \times d} \quad (24)$$

$$C_{air} = C_{air}^0$$

$$\frac{d(C_{cavity})}{dt} = \frac{D_e (C_{air}^0)}{L (\epsilon_b + K') \times d} - \frac{D_e (C_{cavity})}{L (\epsilon_b + K') \times d}$$

Solution to differential equation 28,

$$C_{cavity} = C_{cavity}^0 e^{-at} + C_{air}^0 (1 - e^{-at}) \quad (25)$$

$$\text{Where, } a = \frac{D_e}{L (\epsilon_b + K') d} \quad (30)$$

### **3.2.3.1.2 Phase 2: Reemission of methamphetamine into building**

A mass balance on a simple building see Figure 1.5, subject to a dynamically changing emission rate and constant ventilation is given by the following,

$$V \frac{d C_{air}}{dt} = E(t) - Q C_{air} \quad (31)$$

Where,

$Q$  - is the ventilation rate (or infiltration rate) of a well-mixed house, m<sup>3</sup>/sec

Emission rate is due to flux from walls, (desorption associated with the paint film or other surfaces is neglected in this analysis)

$$E(t) = \frac{-D_e}{L} (C_{air} - C_{cavity}) \times A$$

In this case both  $C_{air}$  and  $C_{cavity}$  are functions of time.

Therefore,

$$V \frac{d C_{air}}{dt} = \left( \frac{-D_e}{L} (C_{air} - C_{cavity}) \times A \right) - Q C_{air}$$

$$\frac{d C_{air}}{dt} = \left( \frac{-D_e}{LV} - \frac{Q}{V} \right) C_{air}(t) + \frac{D_e A}{LV} C_{cavity}(t) \quad (32)$$

The characteristic time for the indoor air concentration to change is approximately equal to  $V/Q$ . This is of the order of  $\sim 1$  hour for a typical house. The characteristic time for a change in the flux through the drywall is  $1/a$  (see equation 30). For the parameters measured in this research, the value ranges from 3 to 1500 days depending on the type of insulation. Thus, the indoor air concentration reaches a rapid pseudo-steady-state relative to air exchange and, over short intervals, the accumulation term in Equation 32,

$$\frac{d C_{air}}{dt} \sim 0.$$

Therefore equation 32 becomes Equation 33,

$$C_{air} = C_{cavity} \left( \frac{\frac{D_e A}{VL}}{\frac{D_e A}{VL} + \frac{Q}{V}} \right) \quad (33)$$

Combining with equation 32 & 33,

$$\frac{d(C_{cavity})}{dt} = \frac{D_e}{L(\epsilon_b + K')d} \left[ \left( \frac{\frac{D_e A}{VL}}{\frac{D_e A}{VL} + \frac{Q}{V}} \right) C_{cavity} - C_{cavity} \right] \quad (34)$$

Solution to Equation 34,

$$C_{cavity} = C_{cavity}^0 e^{-bt} \quad (35)$$

Where,

$$b = \frac{D_e Q}{d(K' + E)(D_e A + QL)}$$

Combining 33 & 35

$$C_{air} = [C_{cavity}^0] \frac{D_e A}{(DA+QL)} e^{-bt} \quad (36)$$

### **3.2.3.1.3 Daily methamphetamine intake and cumulative exposure.**

The daily intake due to inhalation is estimated based on the equation developed by the U.S.EPA, 1989. For noncarcinogenic effects the averaging time (AT) is assumed to be the same as the exposure duration (EFD) (Davis ML et al., 2009, second edition, chapter 6, page 234). Equation 38, is used to estimate a daily dose based on the exposure period of 9 hours for adults and 18 hours for children, under 12 years of age, inside a residence (Kleipis NE, et al., 1996). Table 3.1 tabulates the assumptions for calculating daily inhalation intake.

Table 3.1. Shows the assumptions to calculate the daily inhalation intake

	Body weight <sup>1</sup>	Inhalation rate <sup>1</sup>	Exposure in residence <sup>2</sup>
Adult male	78 kg	15.2 m <sup>3</sup> /day	9 hours
Adult female	65.4 kg	11.3 m <sup>3</sup> /day	9 hours
Child (1-5 years)	16 kg	8.3 m <sup>3</sup> /day	18 hours

<sup>1</sup> Davis ML et al., 2009, second edition, chapter 6 , page 236

<sup>2</sup> Kleipis NE, et al., 1996

Daily intake due to inhalation,

$$I = C \times \frac{CR \times EFD}{BW} \times \frac{1}{AT} \quad (37)$$

Where,

- $I$  - chronic intake,  $\frac{\mu g}{kg \text{ day}}$
- $C$  - chemical air concentration,  $\frac{\mu g}{m^3}$
- $EFD$  - exposure frequency and duration, days
- $CR$  - contact rate, m<sup>3</sup>/day
- $BW$  - body weight, kg
- $AT$  - averaging time, days

Cumulative intake,  $I_{cum}$ , is given by the following equation for time intervals,  $\Delta t$ , that are at constant concentration,

$$I_{cum} = C \times \frac{CR \times EFD}{BW} \times \frac{1}{AT} \times \Delta t \quad (38)$$

## 4. RESULTS

### 4.1. NIBA MEASUREMENTS AND CALIBRATIONS

Since the effective diffusion coefficient is the primary goal of the chamber/flux experiment, these results are presented first. Following this section are the supporting results for method development, calibrations, and chamber validation using water flux through drywall. The results from analytical methods developed include emission rates from diffusion vials, calibrations of dynamic SPME sampler systems to measure the exhaust concentration from the diffusion chamber ( $C_{out}$ ), saturation vapor pressure of commercially available NIBA and saturation concentration ( $C_{saturation}$ ) of NIBA beneath the drywall sample in the diffusion chamber.

**4.1.1. Effective diffusion coefficient ( $D_e$ ).** Figure 4.1 shows the dynamic chamber concentration profiles for samples U1, U3, P1 and P2. After installing the sealed cup in the chamber, the exhaust concentration is near zero and remains low for approximately 50 to 100 hours. The concentration then rises to a steady-state concentration over a 100-200 hour period. Thus, resistance to transport is substantial and penetration through drywall takes several days. Samples U1 and P1 are unpainted and painted versions, respectively, of the same drywall material, hence their behavior can be compared to qualitatively understand the impact of the painted layer. Breakthrough time and time to rise to steady-state appears to be nearly identical. This, phenomena within the drywall itself, such as accumulation and chemistry, appear to dominate the delay in transport. The final steady-state concentration is lower for the painted drywall, indicating reduced flux and increased resistance due to the paint layer.

The measured effective diffusion coefficient for samples U1, U3, P1 and P2 are shown in Table 4.1. The effective diffusivities range over approximately one order of magnitude. Samples U1 and P1 are made of same drywall and hence their diffusion coefficients can be compared to estimate the effective diffusivity of the paint layer of L1. The resistance to diffusion offered by painted drywall is five times the resistance offered by the unpainted drywall. Paint may reduce diffusivity by reducing the effective pore area for flux and by acting as a sorptive sink (adsorption and/or absorption). The calculated



effective diffusion coefficient of paint film is  $2.97 \times 10^{-9} \text{ m}^2/\text{s}$ . Thus methamphetamine accumulation in paint is possible but it is not quantified in this research.

Table 4.1. Steady state flux and effective diffusion coefficient for drywall and painted drywall samples

Sample	Flow through chamber, steady state concentration $C_{out}$ , $\mu\text{g}/\text{m}^3$	Diffusion coefficient $D_e$ , $\text{m}^2/\text{s}$	Steady state flux, $\mu\text{g}/\text{m}^2 \text{ s}$
U1	$27000 \pm 1300$	$7.3 \pm 2.3 \times 10^{-7}$	$51 \pm 3$
U3	$22000 \pm 8400$	$1.2 \pm 0.5 \times 10^{-8}$	$4 \pm 2$
P1	$13000 \pm 6000$	$2.1 \pm 1.4 \times 10^{-7}$	$25 \pm 11$
P2	$5400 \pm 360$	$2.7 \pm 0.4 \times 10^{-8}$	$10 \pm 0.7$
L1		$2.97 \times 10^{-9}$	

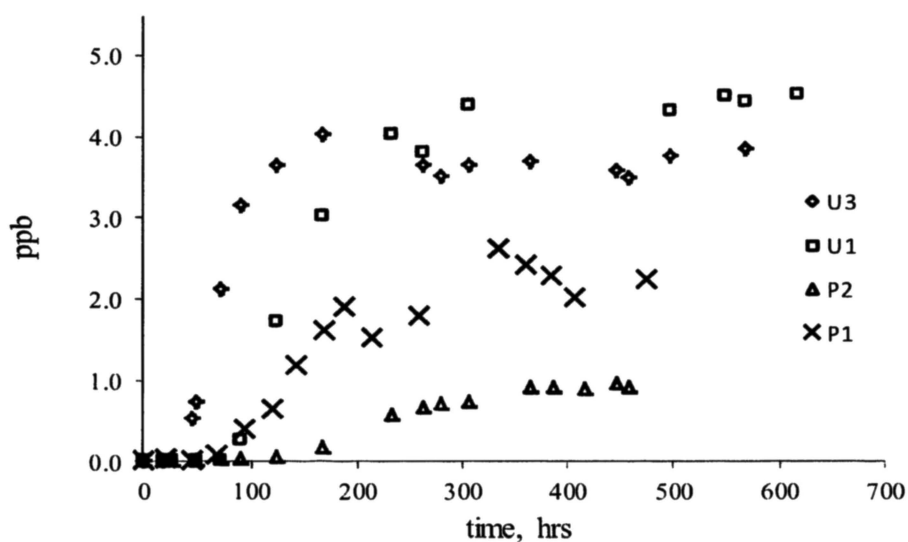


Figure 4.1. Dynamic concentration profile inside the flow through chamber

**4.1.2. Emission rates from gas phase standard systems.** The emission rate of NIBA from 2mm and 5mm diffusion vial is measured. A comparison of low range and high range system is shown in table 4.1. Figure 4.2 and 4.3 shows the decrease in mass of NIBA measured gravimetrically.

Table 4.2. Comparison of low range and high range system

	Vial	Capillary diameter, mm	Temperature inside the bottle, °C	Emission rate $E$ , ng/min	Flow rate $Q$ , L/min	Concentration, $C_{out}$ , $\mu\text{g}/\text{m}^3$
Low range	V1	2mm	35°C	43	$0.105 \pm 0.001$	$84 \pm 12$
High range	V2	5mm	35°C	426	$0.172 \pm 0.007$	$406 \pm 19$

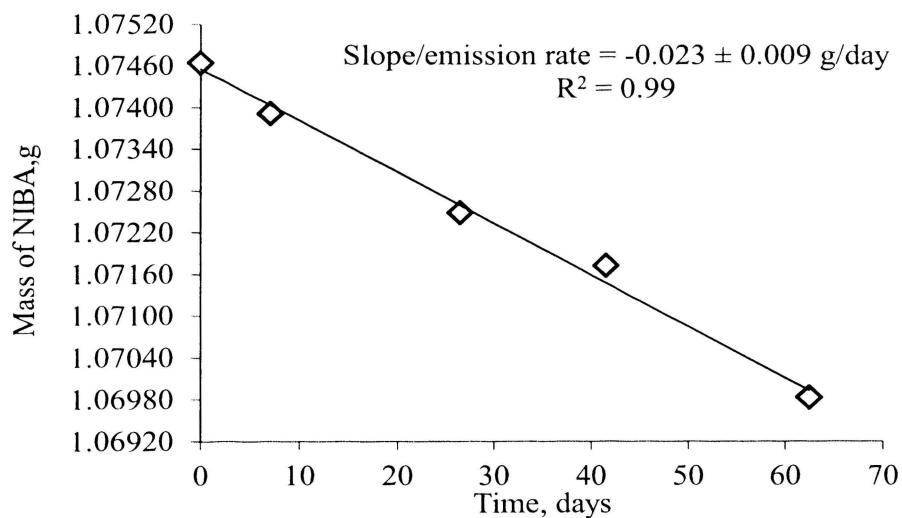


Figure 4.2. Mass of NIBA in V1 vs time

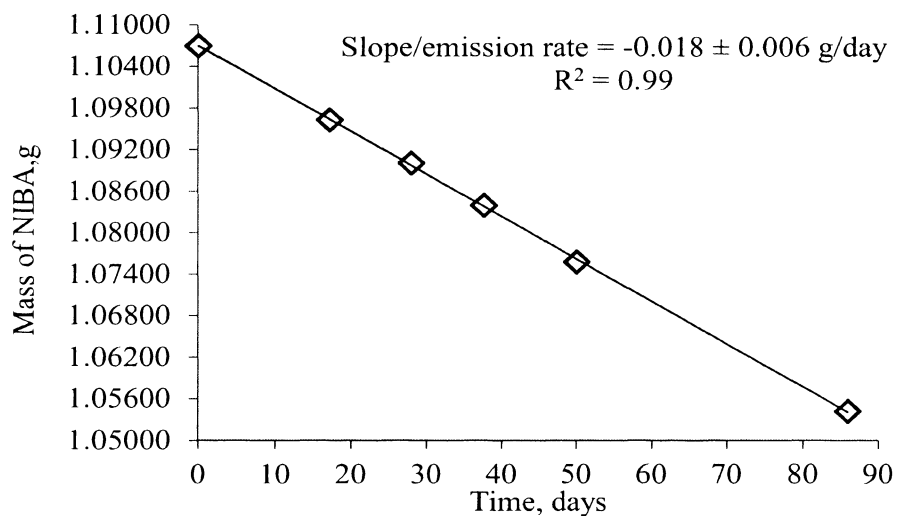


Figure 4.3. Mass of NIBA in V2 vs time

**4.1.3. Calibrating SPME for low range diffusion system.** Shown in Figure 4.4 are the results of a time-weighted calibration of SPME using the low concentration range sampler and the dynamic sampler as shown in Figure 4.1. SPME response is linear over the sampling time range from 1 to 5 minutes.

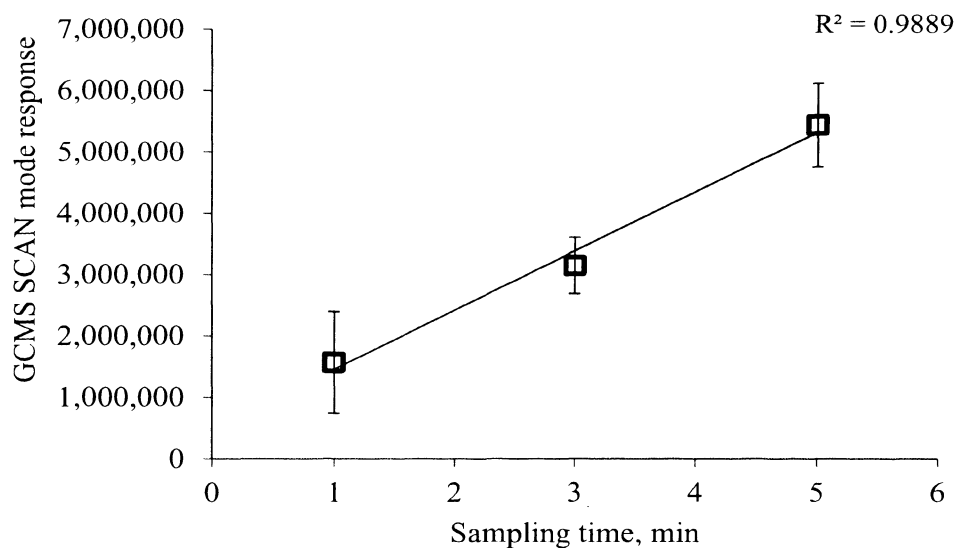


Figure 4.4. GCMS SCAN-mode response for low-concentration ( $84 \pm 12$  ppb) calibration system.

**4.1.4. Calibrating SPME for high range diffusion system.** Shown in Figure 4.5 are the results of a time-weighted calibration SPME using the high concentration range Dynacalibrator system ( $406 \pm 19$  ppb). SPME response is linear over the sampling time range from 0.5 to 5 minutes.

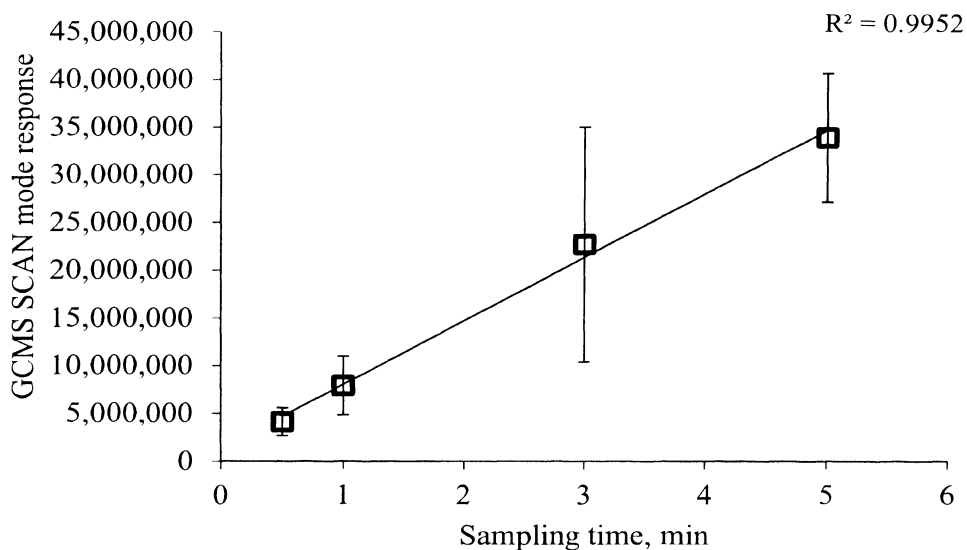


Figure.4.5. GCMS SCAN-mode response for high-concentration ( $406 \pm 19$  ppb) calibration system.

**4.1.5. Validating the setup using diffusion of water.** Water was used in the diffusion flask to validate the diffusion chamber. Water vapor permeability values obtained from literature were used to calculate the diffusion coefficients of plain gypsum board and latex painted gypsum board (see section 3.2.2.9.1). The permeability values reported were  $3.3 \times 10^{-8}$  g /m s pa for gypsum board (Marc and Katia, 2008, pg. 399) and  $2.4 \times 10^{-7}$  g /m<sup>2</sup> s pa (Kumaran, M.K, 2006). Table 4.3 shows the comparison of diffusion coefficients calculated using literature values and the results of diffusion measurements for samples U3 and P2, using pure water in the diffusion flask instead of NIBA. The experimental results are similar in magnitude to that in literature reports and approximately 10 times greater than the diffusion coefficients measured for NIBA.

Table 4.3. Tabulated values of diffusion coefficients of water in literature and actual experiment

	Diffusion coefficient, m <sup>2</sup> /s
Gypsum board <sup>a</sup>	4.4 x 10 <sup>-6</sup>
Plain drywall, Sample U3	3.0 x 10 <sup>-6</sup>
Latex painted gypsum board <sup>b</sup>	2.3 x 10 <sup>-6</sup>
Painted drywall, Sample P2	5.6 x 10 <sup>-7</sup>

<sup>a</sup> Marc and Katia, 2008, pg. 399

<sup>b</sup> Kumaran, M.K, 2006

Plain drywall (U3) and latex painted drywall (P2) were used to validate the system for water.

**4.1.6. NIBA - drywall chemistry.** As the NIBA diffused through the drywall samples, large peaks of benzaldehyde were initially observed, followed by the NIBA peaks. Hypothetically, benzaldehyde was formed as a product of chemistry between NIBA and water, catalyzed by drywall. The precise chemical mechanism that would generate benzaldehyde was not identified, but an acid-catalyzed mechanism that interconverts imines and carbonyls is shown in Figure 4.6. If methamphetamine follows similar hydrolysis pathways, exposure to drywall could reduce methamphetamine concentrations and form a ketone (benzylpropanone), formaldehyde and amines.

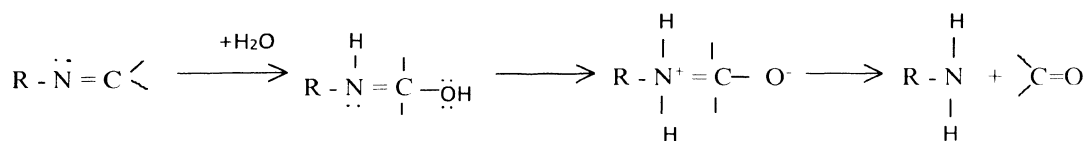


Figure 4.6. Reaction mechanisms from imines to carbonyls

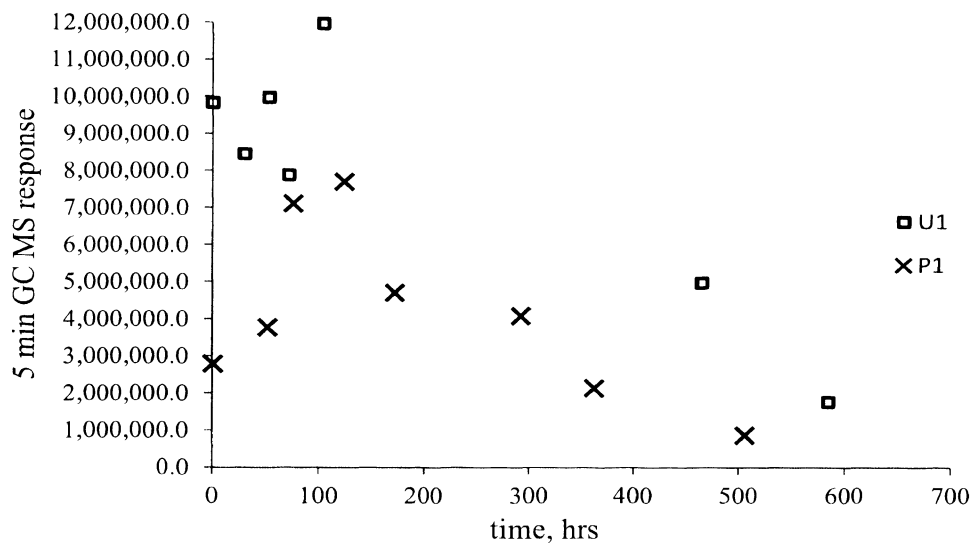


Figure 4.7. Response for benzaldehyde using SPME

**4.1.7. Vapor pressure of pure NIBA.** The measured vapor pressure of NIBA from the saturator was  $523 \pm 60$  ppm. Using equation 19 & 20 from section 3.2, the vapor pressure of NIBA was calculated using the mass collected on a Tenax tube in a known volume of gas from the saturator. Fig 4.8 & Fig 4.9 shows a linear response for different volumes of samples injected from saturator and also different mass injected from the Dynacalibrator.

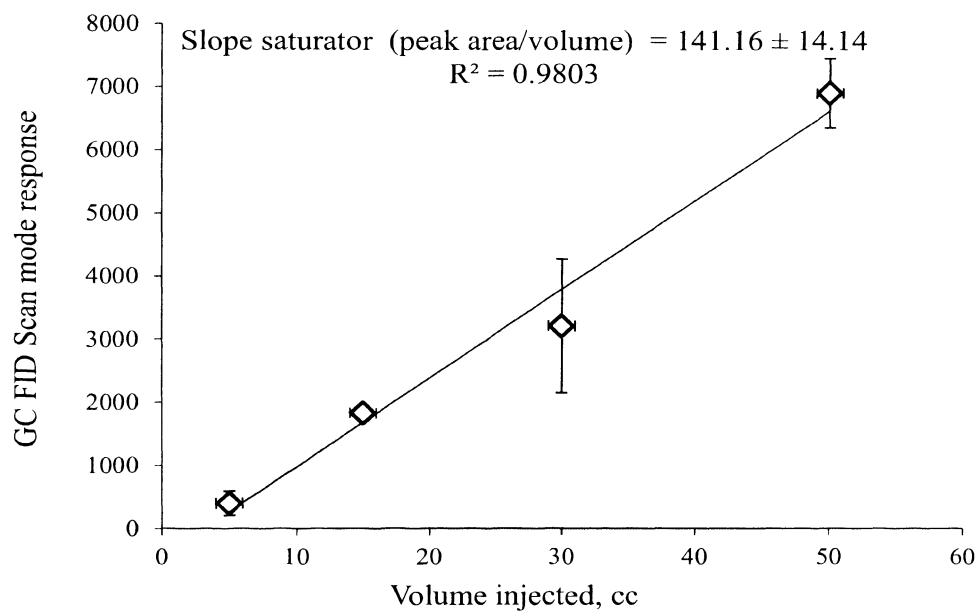


Figure 4.8. Peak area vs volume injected from saturator

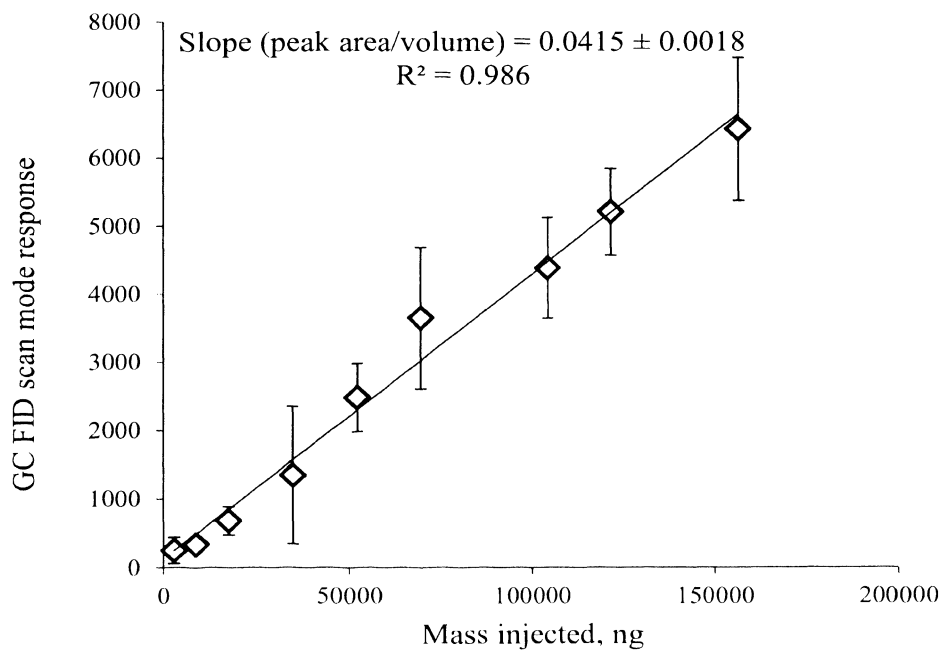


Figure 4.9. Peak area vs mass injected from Dynacalibrator



**4.1.8. Saturation concentration beneath the drywall.** The concentration of NIBA beneath the drywall was determined by inserting the SPME fiber through the drywall once the diffusion system had reached steady state. This static measurement was compared against static measurements of saturated NIBA in a glass bottle (See section 3.2.4 ). The saturation concentration ( $C_s$ ) of NIBA beneath the drywall in diffusion vessel at steady state was  $114 \pm 43$  ppm for U1 and  $186 \pm 76$  ppm for P1. This method had not been developed when P2 and U3 were studied in the NIBA diffusion chamber. For those materials, the diffusion coefficient was calculated using the average  $C_s$  value obtained from U1 and P1 experiments. The saturation concentration of NIBA beneath samples U1 and P1 is about 30% of saturation concentration of pure NIBA, suggesting that the sample purity was reduced after the 500-700 hour duration of the experiment required to achieve steady state.

**4.1.9. Partition coefficient in insulation.** The partition coefficient of NIBA in two types of insulation are tabulated in Table 4.4. By hypothesis 2, the partitioning to cellulose fiber is expected to be greater than fiber glass. Thus it is expected that methamphetamine has high partitioning to cellulose insulation as well. Figure 4.10 shows the bar graph representing the partition coefficients of 10% NIBA in insulation.

Table 4.4. Equilibrium partition coefficient  $K'$

Sample	$(K' = C_{\text{insulation}} / C_{\text{air}})$
<u>Fiber glass</u>	
R-13	$240 \pm 56$
R-30	$180 \pm 98$
Cellulose fiber	$21000 \pm 1500$

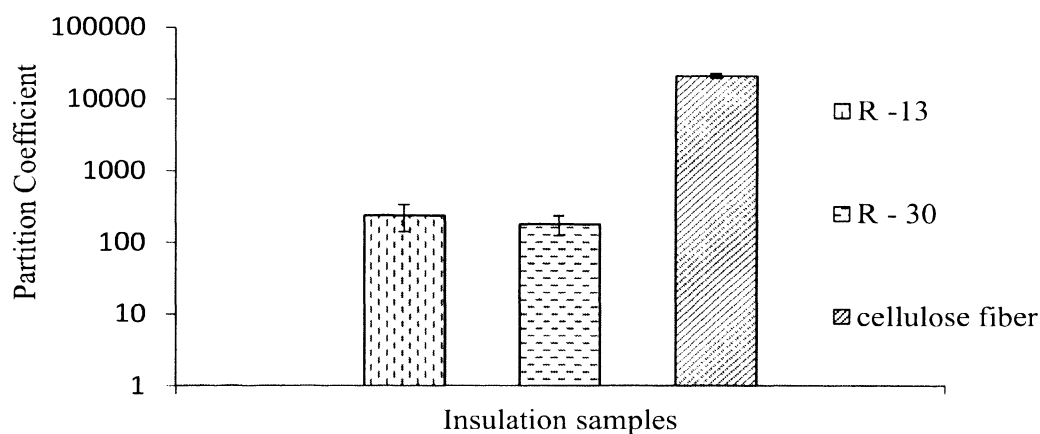


Figure 4.10. Partition coefficients for 10% NIBA equilibration

#### 4.2. MODELING THE ACCUMULATION AND DECAY PHASE OF METHAMPHETAMINE INDOORS

Painted drywall has been shown by this research to be fairly permeable to methamphetamine, with diffusivities only about 10 times lower than that for water. Given sufficient exposure to methamphetamine during illegal production activities, methamphetamine can penetrate through drywall and accumulate in the insulation of wall cavities. To estimate the magnitude of this effect, the diffusivities and insulation partition coefficients are incorporated into a simulation of accumulation (during the cooking process) and re-emission (after cooking, or perhaps after re-occupation). Assuming the methamphetamine free base concentration to be 0.1% of saturation concentration in air during the cooking process, the simulation results reflect the possible contamination of methamphetamine in insulation. The re-emission model predicts the time required for methamphetamine concentrations to decrease to safe levels.

**4.2.1. Accumulation phase.** The simulated accumulation of methamphetamine after 2 weeks in insulation is tabulated for unpainted and latex painted drywall in table 4.5. Figure 4.11 & 4.12 shows the simulated accumulation for a period of two weeks. Since cellulose has a much higher partition coefficient the resulting accumulation is about five times higher than for fiber glass in case of unpainted drywall. Painted drywall has a lower diffusion coefficient, therefore, less accumulates in either insulation material. The partition coefficient is less important as the resistance to transport controls the flux. For a higher diffusion coefficient, resistance to accumulation on the fiberglass insulation (i.e. it begins to saturate) starts to become important.

Table 4.5. Methamphetamine accumulation in insulation

Accumulation of methamphetamine in 163 m <sup>2</sup> surface area	Meth in Cellulose, g	Meth in Fiber glass, g
Drywall	49	10
Painted drywall	13	7

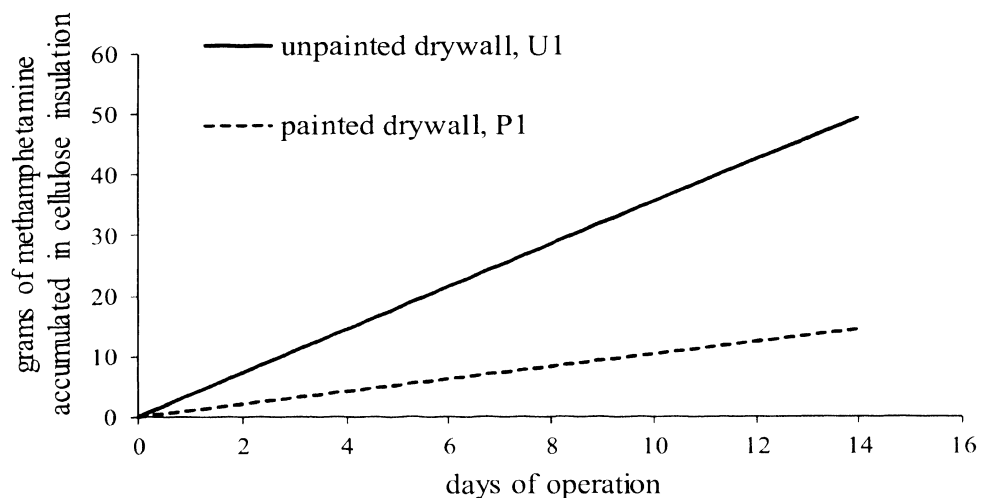


Figure 4.11. Simulated accumulation in cellulose insulation for a period of two weeks operation

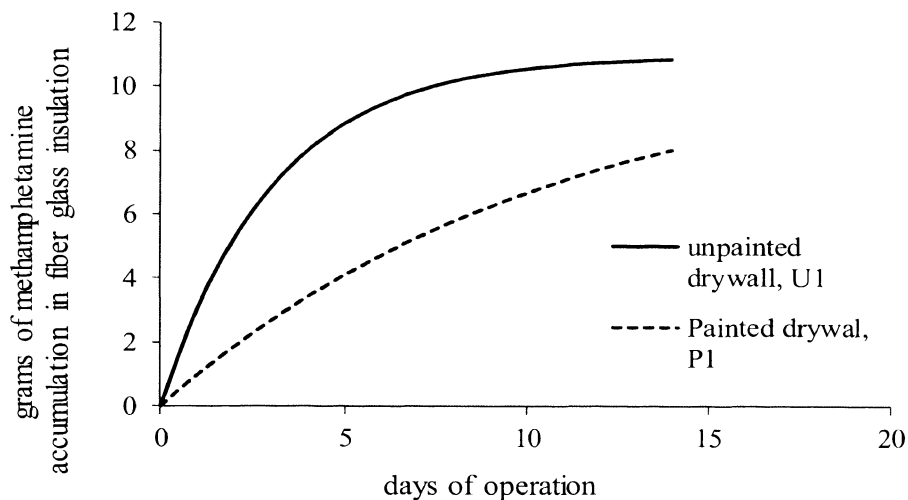


Figure 4.12. Simulated accumulation in fiber glass insulation for two weeks operation

**4.2.2. Release phase.** The elevated indoor concentration due to meth production results in methamphetamine diffusion through the wall assembly and contamination of the insulation. After this accumulation, the building is ventilated and the concentration in the building is much less than that in the air of the wall cavity. Therefore, the chemical driving force results in re-emission into the building. The decay model (described in section 3.2.6.1.2) simulates the dynamic indoor concentration and the time taken to reach safe concentration (RfD) of methamphetamine indoors. These dynamic simulations are shown in Figures 4.13 and 4.14. Because fiberglass accumulates much less methamphetamine, the time required to reach the (RfD) is much lower than for cellulose. The simulation predicts that it will take years to reduce indoor concentrations to safe levels if cellulose insulation is contaminated, regardless of the type of drywall. In the case of fiber glass insulation the concentration reduces to 0.2 ppb within months.

Table 4.6. Time required to reduce indoor concentrations to safe levels during the release phase

Decay phase	Cellulose	Fiber glass
Drywall	7 yrs	66 days
Painted drywall	8 yrs	138 days

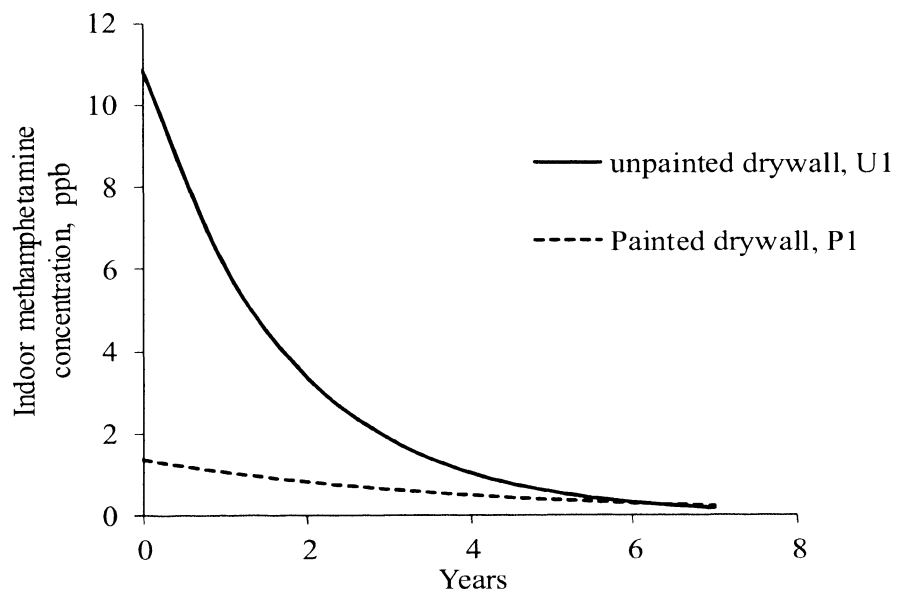


Figure 4.13. Simulated concentrations in room due to emissions from cellulose insulation through drywall

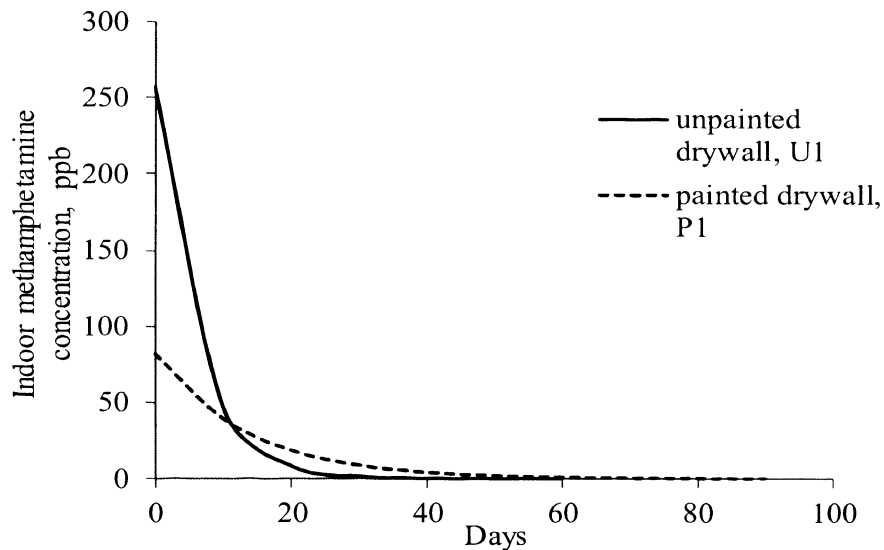


Figure 4.14. Shows the decay phase due to fiberglass installation

The cleanup standard used to determine the minimum dose necessary for children assumes that the air concentrations in methamphetamine labs are dissipated as the labs are remediated. But the results from the release phase model shows that there is likely to be a considerable amount of methamphetamine in air long after re-occupation.

**4.2.3. Daily intake due to inhalation.** The daily intake due to methamphetamine concentration in air during the release phase is shown in the Figure 4.15 - 4.18. As the concentration in the air decreases, the daily intake decreases and reaches the  $0.3 \mu\text{g}/\text{kg}/\text{day}$  reference dose for methamphetamine.

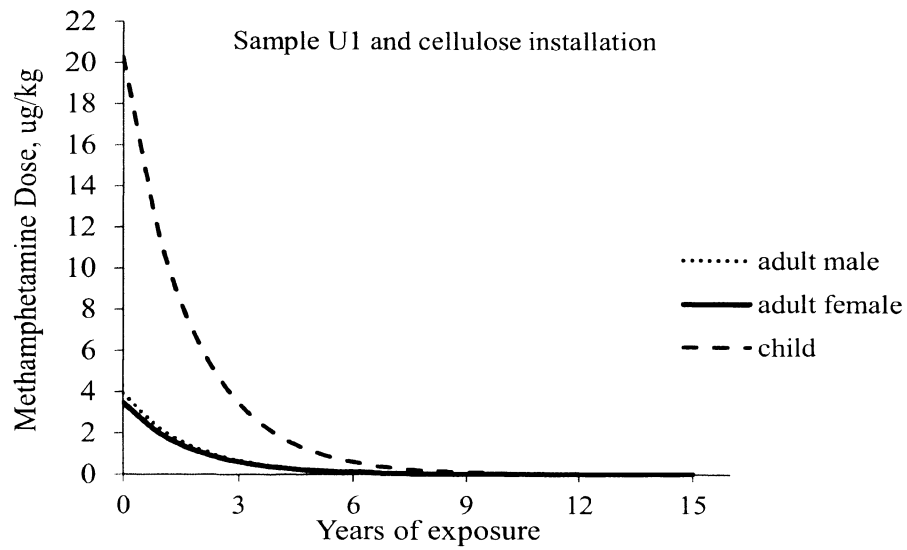


Figure 4.15. Daily dose due emissions from unpainted drywall and cellulose insulation

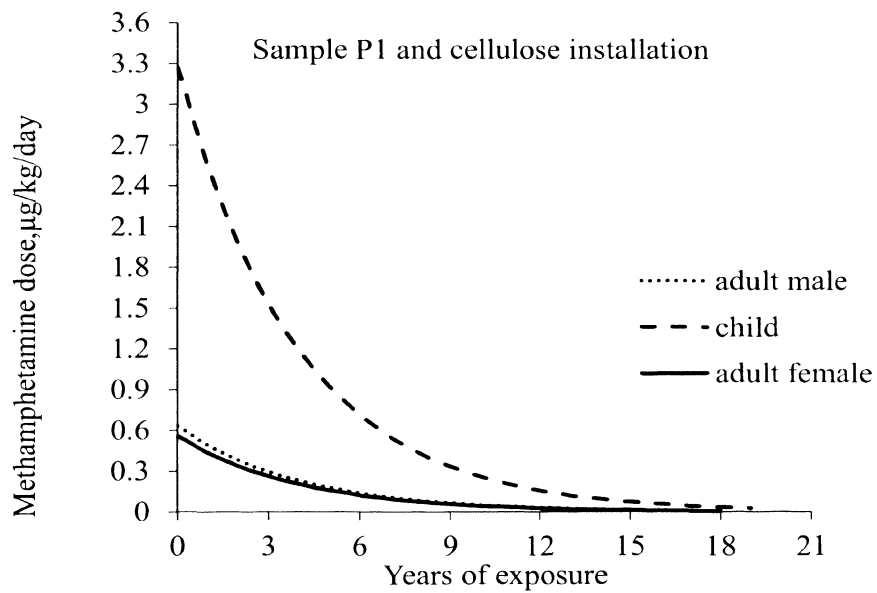


Figure 4.16. Daily dose due to emissions from painted drywall and cellulose insulation

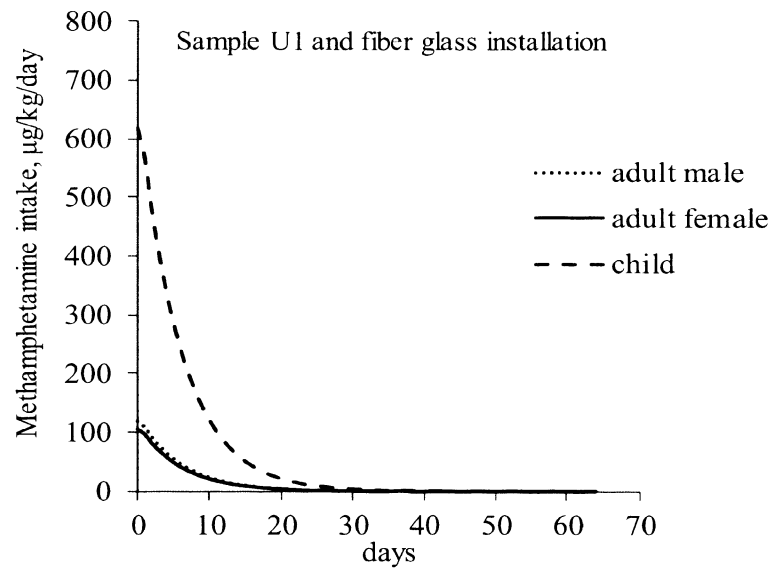


Figure 4.17. Daily dose due to emissions from unpainted drywall and fiberglass insulation

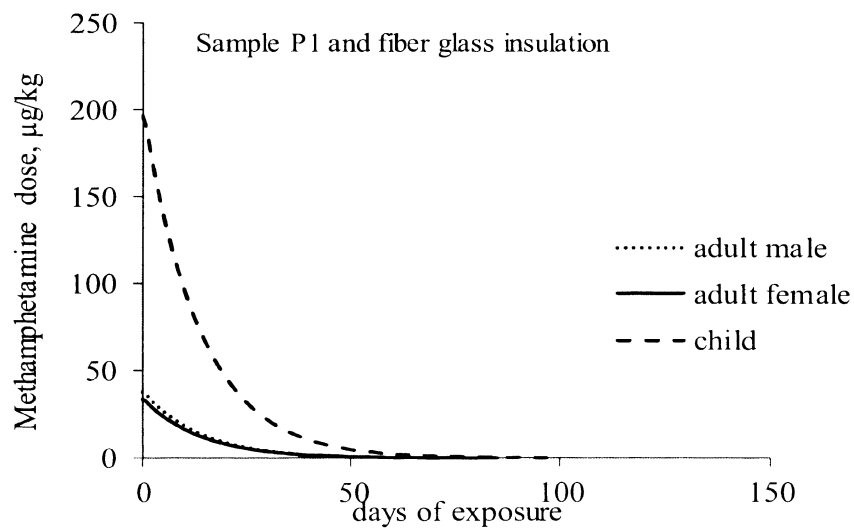


Figure 4.18. Daily dose due to emissions from painted drywall and fiber glass insulation



The dose for a child remains high for either of the wall assembly and two types of insulation as compared to adult male and female. The daily dose for cellulose insulation is 20 times lower than the fiber glass installation with unpainted drywall as the wall assembly. In case of painted drywall, the dose is 50 to 100 times lower for cellulose when compared to fiber glass insulation.

**4.2.4. Cumulative dose.** The cumulative dose for the wall assemblies and the types of insulation is shown in table 4.7.

Table 4.7. Cumulative dose of methamphetamine during reemission period

	Cellulose insulation		Fiber glass insulation	
	U1, $\mu\text{g}/\text{kg}$	P1, $\mu\text{g}/\text{kg}$	U1, $\mu\text{g}/\text{kg}$	P1, $\mu\text{g}/\text{kg}$
Adult male	4953	1070	2042	1000
Adult fe- male	4460	930	1811	887
Child	26097	5841	10594	5185

## 5. CONCLUSIONS AND PRACTICAL IMPLICATIONS

### 5.1. SUMMARY OF EXPERIMENTAL RESULTS

Illegal methamphetamine preparation results in contamination of many surfaces in the indoor environments. From furniture to wall assemblies, methamphetamine has the potential to diffuse into and accumulate in any available and sufficiently porous material. This research shows that a surrogate for methamphetamine can diffuse into and through latex painted drywall. The effective diffusion coefficient measured for the surrogate is about 10 times lower than for water and ranges from  $0.1 \times 10^{-7}$  to  $7 \times 10^{-7} \text{ m}^2 \text{ s}^{-1}$  for several drywall samples. One sample of paint (L1) acts as a partial barrier to methamphetamine with an effective diffusion coefficient about 250 times smaller than unpainted drywall (U1). The resistance due to the paint film could be due to limited porosity but also could indicate sorptive accumulation in paint which might be released into the indoor environment. Insulation in wall cavities can adsorb and accumulate methamphetamine. The partition coefficient for the surrogate measured for the cavity insulation ranged from 190 for fiberglass insulation to 21000 for cellulose insulation at 25 °C.

### 5.2. PRACTICAL IMPLICATIONS

The effective diffusion coefficients and the partition coefficients were used to model the transport through drywall and accumulation in insulation during a 2 week “cook” in a house of typical dimensions and with a typical air exchange rate. Also simulated were the subsequent release of methamphetamine into the residence, the indoor concentrations and the occupant exposure/dose. The accumulation of methamphetamine ranged from about 15-50 grams for cellulose insulation and about 3-10 grams for fiberglass. While fiberglass approached saturation in the two week simulation, cellulose did not. Thus houses with cellulose insulation may have a very high capacity for methamphetamine if illegal methamphetamine production activities take place over a long period of time. Indoor concentrations during the release phase from cellulose insulation remain above a safe level for 3 – 5 years based on the reference dose for adults. The concentration is higher than the safe level for 7 – 10 years for children below the age of 12 years. The concentration drops much more quickly for fiberglass insulation, exposing occupants

to unsafe concentrations for months instead of years, but the initial concentrations (and daily doses) are much higher than for emissions from cellulose insulation.

### 5.3. CONCLUSIONS

The experiments carried out with a methamphetamine surrogate in this research suggest that methamphetamine can diffuse through painted walls and contaminate material inside wall cavities. This contamination can act as a long-term source of exposure to occupants of former meth-labs. Contamination of materials inside wall cavities is not considered in voluntary clean up guidelines. Future guidelines should reconsider simply cleaning surfaces and consider full removal of the cavity insulation and drywall. During remediation the presampling results are relied upon to identify which rooms to clean. The results of this research suggest that other rooms may be at risk because methamphetamine vapor can penetrate through wall assemblies.

The long breakthrough time and the relatively large resistance to diffusion between unpainted and painted drywall suggests that methamphetamine can accumulate in paint itself and even if a vapor barrier is installed, paint itself could be a significant reservoir. This accumulation of methamphetamine in paint will contribute to even more available methamphetamine and a potentially higher dose for occupants. Encapsulating walls, ceilings and floors with a low-permeability paint is listed as an option in the remediation guidelines. But the impact this may have on preventing methamphetamine from diffusing out of the underlying paint layer or from the wall cavity is unclear. Further, wall penetrations (such as electrical outlets) may become the primary route of emission, thus reducing the effectiveness of encapsulation, at least in preventing cavity contamination from entering the room.

Although only one chemical and a limited range of materials were tested, the research suggests that chemicals of similar volatility, and/or chemical structure, could also penetrate and accumulate in wall cavities. Thus, exposure to hazardous volatile, or semi-volatile, chemicals associated with construction or remodeling could be extended much longer than anticipated after airing out the building. Nicotine is a structurally similar species: is it possible that it also penetrates and accumulates in wall cavities? Environmental Tobacco Smoke (ETS) is comprised of gas and condensed tar

particles. The gases include, alkenes, nitrosamines, aromatic and heterocyclic hydrocarbons and amines. There are no reported studies on the diffusion of ETS gases through and into wall assemblies, but the research reported here can be used to initiate an “order-of-magnitude” analysis of walls as a long-term source of exposure.

## **6. FUTURE RESEARCH**

### **6.1. BUILDINGS AND BUILDING MATERIALS**

Apart from the wall assemblies made of drywall, different types of paint, wood and manufactured wood products, insulation should also be considered for performing diffusion and accumulation experiments. Since this research focused only on drywall, the result of considering a variety of materials, with different material properties will be to provide more information for a better model of the long term emissions rates in a building as a whole after a cooking episode. Also, the impact of sorption to newly installed materials such as carpet, furniture and clothing should also be considered.

There are a wide variety of building types that may become contaminated. In addition to traditional single-family houses, this research should also consider the impact on manufactured homes, mobile homes, hotel rooms, multi-family dwellings and apartments.

### **6.2. CHEMISTRY OF BUILDING MATERIALS**

At the initial period of the diffusion experiments, SPME samples were collected immediately after introducing the NIBA beneath the material samples. The analysed samples showed benzaldehyde peaks due to possible hydrolysis chemistry involving water (50% relative humidity) NIBA and drywall. It is not yet clear if methamphetamine will also be subject to this hydrolysis chemistry. Designing experiments to study about the kinetics of this reaction, and the products formed, might reveal if drywall can be used to more rapidly remove methamphetamine from contaminated homes.

### **6.3. DIFFUSION EXPERIMENTS AT LOWER CONCENTRATIONS**

For the cup method in this research, pure NIBA was used to generate a saturation concentration beneath the drywall samples. It will be valuable to perform diffusion experiments with lower concentration NIBA solutions, and also low-concentration methamphetamine solutions, to simulate the lower-concentration conditions, of free-base meth, typical of illegal lab environments.

APPENDIX A.  
TABULATED EXPERIMENTAL VALUES

Table A1. Showing the dynamic  $C_{out}$  in flow through chamber for NIBA in sample U1

Hours	Response in GC	$\mu\text{g}/\text{m}^3$	ppb	ppm
1	11439	1	0.14	0.0001
20	703475	51	8.37	0.008
27	304398	22	3.62	0.004
51	237093	17	2.82	0.003
73	625015	45	7	0.007
92	22062300	1601	263	0.263
125	144319566	10472	1717	1.717
169	252290191	18307	3002	3.002
235	337529790	24492	4017	4.017
264	318075624	23081	3785	3.785
308	366711040	26610	4364	4.364
499	361786612	26253	4305	4.305
552	376093115	27291	4476	4.476
571	370438440	26880	4408	4.408
620	378375280	27456	4503	4.503

Table A2. Showing the estimated  $D_e$  for NIBA in sample U1

<b>Response for 5min from standard</b>	13782 $\pm$ 2809
<b><math>C_{outs}</math> steady state, <math>\mu\text{g}/\text{m}^3</math></b>	27454 $\pm$ 1364
<b>Diameter of the sample U1, m</b>	0.15
<b>Surface area of sample, <math>\text{m}^2</math></b>	0.02
<b>Thickness of U1, m</b>	0.01 $\pm$ 0.0005
<b>Saturation concentration, <math>C_s</math>, <math>\mu\text{g}/\text{m}^3</math></b>	733545 $\pm$ 218995
<b>Flow rate in chamber, <math>Q</math>, <math>\text{m}^3/\text{s}</math></b>	0.000033
<b>Steady state flux, <math>\mu\text{g}/\text{m}^2 \text{ s}</math></b>	51 $\pm$ 3
<b><math>(C_s - C_{out})</math>, <math>\mu\text{g}/\text{m}^3</math></b>	706091 $\pm$ 213697
<b>Diffusion coefficient in U1, <math>D_e</math>, <math>\text{m}^2/\text{s}</math></b>	7.26E-07 $\pm$ 2.26 E-07

Table A3. Showing the dynamic  $C_{out}$  in flow through chamber for NIBA in sample P1

Hours	Response	$\mu\text{g}/\text{m}^3$	ppb	ppm
1	394574	49	8	0.0081
23	2221064	161	26	0.026
47	1498020	109	18	0.018
68.7	5900272	428	70	0.070
		0	0	
170	133745361	9705	1592	1.6
189	158095949	11472	1881	1.9
216	126499879	9179	1505	1.5
260	150356862	10910	1789	1.8
336	219085779	15898	2607	2.6
362	202374754	14685	2408	2.4
387	190612108	13832	2268	2.3
409.5	167517629	12156	1994	2.0
553	136843895	9930	1629	1.6

Table A4. Showing the estimated  $D_e$  for NIBA in sample P1

<b>Response for 5min from standard</b>	13782 $\pm$ 2809
$C_{out}$ , steady state, $\mu\text{g}/\text{m}^3$	22161 $\pm$ 5778
Diameter of the sample U1, m	0.15
Surface area of sample, $A$ $\text{m}^2$	0.02
Thickness of U1, m	0.01 $\pm$ 0.0005
Saturation concentration, $C_s$ , $\mu\text{g}/\text{m}^3$	1192525 $\pm$ 361656
Flow rate in chamber, $Q$ , $\text{m}^3/\text{s}$	0.000033
Steady state flux, $\text{ug}/\text{m}^2 \text{ s}$	25 $\pm$ 11
$(C_s - C_{out})$ , $\mu\text{g}/\text{m}^3$	1179190 $\pm$ 623642
Diffusion coefficient in U1, $D_e$ , $\text{m}^2/\text{s}$	2.11E-07 $\pm$ 1.44E-07



Table A5. Showing the dynamic  $C_{out}$  in flow through chamber for NIBA in sample U3

Hours	Response	$\mu\text{g}/\text{m}^3$	ppb	ppm
1	109333	7.8	1.28	0.001
20	270000	19.3	3.16	0.003
47	45200000	3229	529	0.53
51	61792553	4414	724	0.72
73	181049210	12932	2121	2.12
92	268863065	19205	3150	3.15
125	310903300	22207	3642	3.64
169	343427274	24531	4023	4.02
264	309534904	22110	3626	3.63
282	299368995	21383	3507	3.51
308	309359905	22097	3624	3.62
366	314790000	22485	3688	3.69
448	304358601	21740	3565	3.57
460	297699220	21264	3487	3.49
499	318955941	22783	3736	3.74
571	328052188	23432	3843	3.84

Table A6. Showing the estimated  $D_e$  for NIBA in sample U3

<b>Response for 5min from standard</b>	14000 $\pm$ 5200
<b><math>C_{outs}</math> steady state, <math>\mu\text{g}/\text{m}^3</math></b>	22161 $\pm$ 8409
<b>Diameter of the sample U1, m</b>	0.15
<b>Surface area of sample, <math>A</math> <math>\text{m}^2</math></b>	0.02
<b>Thickness of U1, m</b>	0.01 $\pm$ 0.0005
<b>Saturation concentration, <math>C_s</math>, <math>\mu\text{g}/\text{m}^3</math></b>	3353658 $\pm$ 365854
<b>Flow rate in chamber, <math>Q</math>, <math>\text{m}^3/\text{s}</math></b>	0.000033
<b>Steady state flux, <math>\text{ug}/\text{m}^2 \text{ s}</math></b>	4 $\pm$ 2
<b><math>(C_s - C_{out})</math>, <math>\mu\text{g}/\text{m}^3</math></b>	3331496 $\pm$ 365950
<b>Diffusion coefficient in U1, <math>D_e</math>, <math>\text{m}^2/\text{s}</math></b>	1.24E-08 $\pm$ 0.49-08

Table A7. Showing the dynamic  $C_{out}$  in flow through chamber for NIBA in sample P2

Hours	Response	$\mu\text{g}/\text{m}^3$	ppb	ppm
1	628102	46	7	0.007
20	612099	44	7	0.007
27	620682	45	7	0.007
51	1437473	104	17	0.017
73	2570338	187	31	0.031
92	3448778	250	41	0.041
125	5460452	396	65	0.065
169	14369569	1043	171	0.171
235	48122887	3492	573	0.573
264	54607095	3962	650	0.650
282	59327578	4305	706	0.706
308	60746668	4408	723	0.723
366	75432838	5474	898	0.898
388	75540524	5481	899	0.899
419	75070702	5447	893	0.893
448	79431942	5764	945	0.945
460	75434542	5474	898	0.898

Table A8. Showing the estimated  $D_e$  for NIBA in sample P2

<b>Response for 5min from standard</b>	13782 $\pm$ 2809
<b><math>C_{out}</math>, steady state, <math>\mu\text{g}/\text{m}^3</math></b>	5473 $\pm$ 368
<b>Diameter of the sample U1, m</b>	0.15
<b>Surface area of sample, <math>A</math> <math>\text{m}^2</math></b>	0.02
<b>Thickness of U1, m</b>	0.01 $\pm$ 0.0005
<b>Saturation concentration, <math>C_s</math>, <math>\mu\text{g}/\text{m}^3</math></b>	3353658 $\pm$ 365853
<b>Flow rate in chamber, <math>Q</math>, <math>\text{m}^3/\text{s}</math></b>	0.000033
<b>Steady state flux, <math>\mu\text{g}/\text{m}^2 \text{ s}</math></b>	10 $\pm$ 0.6
<b><math>(C_s - C_{out})</math>, <math>\mu\text{g}/\text{m}^3</math></b>	33481185 $\pm$ 428977
<b>Diffusion coefficient in U1, <math>\text{m}^2/\text{s}</math></b>	2.74E-08 $\pm$ 0.39 E-08

Table A9. Showing the dynamic  $C_{out}$  in flow through chamber for Water in sample U3

<b>RH%</b>	<b>hours</b>		<b>pa</b>	<b>kg/m<sup>3</sup></b>	<b><math>C_{out}</math>,g/m<sup>3</sup></b>
0.0	9.9	23087	231	0.0017	1.7
0.2	10.9	25401	254	0.0018	1.8
0.3	10.6	24703	247	0.0018	1.8
0.4	10.2	23773	238	0.0017	1.7
1.0	10.1	23436	234	0.0017	1.7
1.3	10.4	24134	241	0.0018	1.8
4.1	10.8	25064	251	0.0018	1.8
5.2	10.8	24994	250	0.0018	1.8
6.9	11.0	25645	256	0.0019	1.9
10.6	11.4	26459	265	0.0019	1.9
13.6	11.5	26621	266	0.0019	1.9
20.3	11.6	26970	270	0.0020	2.0
29.5	11.5	26807	268	0.0019	1.9
39.7	11.5	26807	268	0.0019	1.9
53.4	11.5	26807	268	0.0019	1.9
62.2	11.6	26970	270	0.0020	2.0
72.07	11.6	26970	270	0.0020	2.0

Table A10. Showing the estimated  $D_e$  based on literature values for Water in sample U3

<b>from literature</b>	
<b>Molecular weight of water, g/mol</b>	18
<b>Gas constant, m<sup>3</sup> pa/ K mol</b>	8.134
<b>Temperature, K</b>	298
<b>Permeability, g m<sup>-1</sup> s<sup>-1</sup> pa<sup>-1</sup></b>	3.28E-08
<b>Diameter of the sample U3, m</b>	0.15
<b>Surface area of sample, m<sup>2</sup></b>	0.018
<b>Thickness of U3, m</b>	0.01
<b>Saturation concentration, <math>C_s</math>, g/m<sup>3</sup></b>	23.00
<b>Flow rate in chamber, <math>Q</math>, m<sup>3</sup>/s</b>	3.30E-05
<b><math>C_{out}</math>, steady state, g/m<sup>3</sup></b>	5.437
<b>Steady state flux, g/m<sup>2</sup> s</b>	1.02E-02
<b>Diffusion coefficient, <math>D_e</math>, m<sup>2</sup>/s</b>	4.42E-06

Table A11. Showing the estimated  $D_e$  from experiment using Water for sample U3

<b>From experiment</b>	
<b><math>C_{out}</math>, steady state, g/m<sup>3</sup></b>	1.93
<b>Diameter of the sample U3, m</b>	0.018
<b>Surface area of sample, m<sup>2</sup></b>	0.010
<b>Thickness of U3, m</b>	0.010
<b>Saturation concentration, <math>C_s</math>, g/m<sup>3</sup></b>	23
<b>Flow rate in chamber, <math>Q</math>, m<sup>3</sup>/s</b>	3.30E-05
<b>Steady state flux</b>	6.37E-03
<b><math>(C_s - C_{out})</math>, g/m<sup>3</sup></b>	21
<b>Diffusion coefficient of water U3, m<sup>2</sup>/s</b>	3.02E-06
<b>Permeability, g m<sup>-1</sup> s<sup>-1</sup> pa<sup>-1</sup></b>	2.24E-08

Table A12. Showing the dynamic  $C_{out}$  in flow through chamber for water in sample P2

<b>RH%</b>	<b>hours</b>		<b>p<sub>a</sub></b>	<b>kg/m<sup>3</sup></b>	<b>g/m<sup>3</sup></b>
1.9	12	4301	43	0.00031	0.3
1.6	16	3778	38	0.00027	0.3
1.4	20	3197	32	0.00023	0.2
1.3	23	3023	30	0.00022	0.2
11.2	24	25924	259	0.00188	1.9
15.8	24	36677	367	0.00266	2.7
17.0	24	39525	395	0.00287	2.9
11.0	24	25575	256	0.00186	1.9
6.0	26	13950	140	0.00101	1.0
5.0	31	11683	117	0.00085	0.8
4.7	36	10928	109	0.00079	0.8
4.4	50	10230	102	0.00074	0.7
4.4	64	10230	102	0.00074	0.7
4.2	83	9823	98	0.00071	0.7
4.4	0	10303	103	0.00075	0.7

Table A13. Showing the estimated  $D_e$  based on literature values for water in sample P2

<b>from literature</b>	
<b>Molecular weight of water, g/mol</b>	18
<b>Gas constant, m<sup>3</sup> pa/ K mol</b>	8.134
<b>Temperature, K</b>	298
<b>Permeability, g m<sup>-1</sup> s<sup>-1</sup> pa<sup>-1</sup></b>	2.46E-06
<b>Diameter of the sample P2, m</b>	0.15
<b>Surface area of sample, m<sup>2</sup></b>	0.018
<b>Thickness of P2, m</b>	0.009
<b>Saturation concentration, C<sub>s</sub>, g/m<sup>3</sup></b>	23.00
<b>Flow rate in chamber, Q, m<sup>3</sup>/s</b>	3.30E-05
<b>C<sub>out</sub>, steady state, g/m<sup>3</sup></b>	4.078
<b>Steady state flux, g/m<sup>2</sup> s</b>	7.62E-03
<b>Diffusion coefficient, D<sub>e</sub>, m<sup>2</sup>/s</b>	2.98E-06

Table A14. Showing the estimated  $D_e$  from experiment using water for sample P2

<b>From experiment</b>	
<b><math>C_{out}</math> steady state, g/m<sup>3</sup></b>	0.74
<b>Diameter of the sample P2, m</b>	0.150
<b>Surface area of sample, m<sup>2</sup></b>	0.018
<b>Thickness of P2, m</b>	0.009
<b>Saturation concentration, <math>C_s</math>, g/m<sup>3</sup></b>	23
<b>Flow rate in chamber, Q, m<sup>3</sup>/s</b>	3.30E-05
<b>Steady state flux</b>	1.38E-03
<b><math>(C_s - C_{out})</math>, g/m<sup>3</sup></b>	22
<b>Diffusion coefficient of water P2, m<sup>2</sup>/s</b>	5.59E-07
<b>Permeability, g m<sup>-1</sup> s<sup>-1</sup> pa<sup>-1</sup></b>	4.61E-07

Table A15. Mass change of NIBA in Vial V1

<b>Mass of empty diffusion vial (2mm)</b>				<b>14.73275</b>	<b>grams</b>
<b>6/15/11, 9.00PM</b>	<b>6/22/11, 10.00PM</b>	<b>7/13/11, 2.50PM</b>	<b>7/27/11, 5.30PM</b>	<b>9/18/11, 1.00PM</b>	
1.07461	1.07397	1.07248	1.07178	1.06989	
1.07462	1.07389	1.07245	1.07178	1.06981	
1.07464	1.07388	1.07244	1.07175	1.06979	
1.07465	1.07392	1.07247	1.07177	1.06984	
1.07465	1.07395	1.07249	1.07174	1.06983	
1.07465	1.07391	1.07249	1.07173	1.06977	
1.07469	1.07392	1.07249	1.07166	1.06981	
1.07465	1.07385	1.07246	1.07167	1.06983	
1.07464	1.07390	1.07251	1.07166	1.06982	
1.07463	1.07390	1.07251	1.07165	1.06986	
1.07464	1.07391	1.07248	1.07172	1.06983	

Table A16. Emission rate of NIBA in Vial V1

<b>Initial weight of NIBA, g</b>	1.07464
<b>Final weight of NIBA, g</b>	1.06983
<b>Emission time, min</b>	89940
<b>Total emission rate, g/min</b>	0.0000000536
<b>Emission rate of NIBA, ng/min</b>	53 ± 8
<b>Flow rate of the setup, L/min</b>	0.105 ± 0.001
<b>C<sub>out</sub>, mass concentration of NIBA, μg/m<sup>3</sup></b>	514 ± 76
<b>C<sub>out</sub>, mixing ratio of NIBA, ppb</b>	84 ± 12
<b>Molecular weight of NIBA, g/mol</b>	149

Table A17. Mass change of NIBA in Vial V2

Mass of empty diffusion vial (5mm)				14.09876	grams
7.11.2011,10.44AM	7.29.2011, 4.40PM	8.9.2011, 12.00PM	8.20.2011, 11.00AM	9.1.2011, 9.20 PM	10.7.2011, 7.34PM
1.10688	1.09623	1.09002	1.08399	1.07582	1.05419
1.10689	1.09627	1.09006	1.08395	1.07577	1.05418
1.10686	1.09622	1.09003	1.08394	1.07572	1.05420
1.10690	1.09621	1.09003	1.08394	1.07578	1.05419
1.10688	1.09627	1.08989	1.08394	1.07572	1.05420
1.10692	1.09618	1.09002	1.08394	1.07574	1.05412
1.10692	1.09628	1.09004	1.08393	1.07572	1.05418
1.10693	1.09623	1.09003	1.08393	1.07573	1.05413
1.10692	1.09628	1.08999	1.08391	1.07572	1.05410
1.10689	1.09626	1.09002	1.08393	1.07571	1.05409
1.10690	1.09624	1.09001	1.08394	1.07574	1.05416

Table A18. Mass change of NIBA in Vial V2

<b>Initial weight of NIBA, g</b>	1.10690
<b>Final weight of NIBA, g</b>	1.05416
<b>Emission time, min</b>	123780
<b>Total emission rate, g/min</b>	0.000000426
<b>Emission rate of NIBA, ng/min</b>	426 ± 10
<b>Flow rate of the setup, L/min</b>	0.172 ± 0.007
<b>C<sub>out</sub>, mass concentration of NIBA, µg/m<sup>3</sup></b>	2463 ± 116
<b>C<sub>out</sub>, mixing ratio of NIBA, ppb</b>	406 ± 19
<b>Molecular weight of NIBA, g/mol</b>	149



Table A20. Volume response for Saturator in FID

Volume, cc		0.00	5.00	15.00	30.00	50.00	
<b>FID Re-</b>		0.00	549.00	1817.00	3079.00	6870.00	2463.00
<b>sponse</b>		0.00	354.00	1786.00	2422.00	6986.00	2309.60
		0.00	368.00	1865.00	3411.00	6894.00	2507.60
		0.00	363.00	1870.00	3451.00	7243.00	2585.40
		0.00	405.00	1760.00	3454.00	6826.00	2489.00
		0.00	360.00	1865.00	3457.00	6590.00	2454.40
	Avg	0.00	399.83	1827.17	3212.33	6901.50	<b>2468.17</b>
	STDV	0.00	75.28	46.92	414.03	213.33	90.66
		0.00	6.00	6.00	6.00	6.00	6.00
		0.00	0.05	0.05	0.05	0.05	0.05
		0.00	2.57	2.57	2.57	2.57	2.57
	CL	0.00	193.51	120.61	1064.29	548.38	<b>233.04</b>

Table A21. Mass response from dynacalibrator

MFC setting,	93	cc/min	
Calibration factor for MFC	1.1654		
Actual MFC flow at 0°C	108	cc/min	
Temperature correction factor	1.0769		
Actual flow, 25°C	116.72	cc/min	
	116.72	ml/min	
Mass concentration from dynacalibrator	2460.00	µg/m <sup>3</sup>	
<b>Sampling time, min</b>	<b>Actual flow, L</b>	<b>Mass injected, ng</b>	<b>FID response</b>
10	1.17	2906	248 ± 191
30	3.50	8719	335 ± 30
60	7.00	17438	684 ± 207
120	14.01	34876	1346 ± 1004
180	21.01	52314	2475 ± 496
240	28.01	69751	3641 ± 1040
360	42.02	104627	4372 ± 738
420	49.02	122065	5196 ± 636
540	63.03	156941	6414 ± 1051
Average			2746 ± 599

Table A22. Calculation of vapor pressure from saturation experiment

<b>Slope from saturator</b>	141 ± 14.14
<b>Slope from dynacalibrator</b>	0.042 ± 0.0018
<b>Saturation concentration of pure NIBA, µg/m<sup>3</sup></b>	3203832 ± 815948
<b>Mixing ratio, ppb</b>	525428 ± 133815
<b>Mixing ratio, ppm</b>	525 ± 133
<b>Vapor pressure, mm Hg</b>	0.399 ± 0.101

Table A23. Saturation concentration beneath the sample U1

<b>SPME response for 100% pure NIBA</b>	164236639 ± 45640976
<b>Saturation concentration measured for NIBA, ppm</b>	550 ± 60
<b>SPME response for U1 beneath drywall</b>	35923490
<b>Saturation mixing ration beneath drywall, ppm</b>	120 ± 36
<b>Corresponding mass concentration, <math>\mu\text{g}/\text{m}^3</math></b>	733546 ± 218995

Table A24. Saturation concentration beneath the sample P1

<b>SPME response for 100% pure NIBA</b>	164236639 ± 45640976
<b>Saturation concentration measured for NIBA, ppm</b>	550 ± 60
<b>SPME response for P1 beneath drywall</b>	58400791
<b>Saturation mixing ration beneath drywall, ppm</b>	196 ± 59
<b>Corresponding mass concentration, <math>\mu\text{g}/\text{m}^3</math></b>	1192525 ± 361656

Table A25. Density of insulation

## Determine Density

Test 1	Mass (g)	Volume (cm <sup>3</sup> )	Density (g/cm <sup>3</sup> )
R-30	2.7393	210	0.013
R-13	2.2763	126.48	0.018
Ceiling Tile	6.5028	29.7	0.219
Natural Fiber	20.0231	300	0.067

Test 2	Mass (g)	Volume (cm <sup>3</sup> )	Density (g/cm <sup>3</sup> )
R-30	1.5345	91.125	0.017
R-13	1.9995	94.25	0.021
Ceiling Tile	12.6887	50.96	0.249
Natural Fiber	21.2141	300	0.071

Test 3	Mass (g)	Volume (cm <sup>3</sup> )	Density (g/cm <sup>3</sup> )
R-30	2.3902	151.25	0.016
R-13	2.0378	122.96	0.017
Ceiling Tile	15.7928	69.3	0.228
Natural Fiber	22.5755	300	0.075

Average	Density (g/cm <sup>3</sup> )
R-30	0.015
R-13	0.019
Ceiling Tile	0.232
Natural Fiber	0.071

Table A26. Partition coefficient of NIBA in fiber glass insulation

	Sample ID	Weight (w/o ins) [1]	Weight (w/ ins) [2]	Weight (of ins) [2-1]	Weight (after) [3]	Δ Weight (g)
	M01	1.08398	1.32425	0.24027	1.32467	0.00042
	M02	1.06379	1.28148	0.21769	1.2819	0.00042
<b>R-13</b>	M03	1.08842	1.39481	0.30639	1.39535	0.00054
	M04	1.09051	1.33746	0.24695	1.33778	0.00032
	M05	1.08872	1.42596	0.33724	1.42633	0.00037
	M06	1.07852	1.38197	0.30345	1.38219	0.00022
	M07	1.09298	1.36909	0.27611	1.36955	0.00046
<b>R-30</b>	M08	1.07129	1.34186	0.27057	1.34224	0.00038
	M09	1.08856	1.41863	0.33007	1.41918	0.00055
	M10	1.09518	1.33772	0.24254	1.33793	0.00021

Weight (equilibration)	Δ Weight (g)	Uptake (g/g)	Cins	K
1.325	0.00075	0.003	5.80E-05	256.88
1.28225	0.00077	0.004	6.58E-05	291.09
1.39569	0.00088	0.003	5.34E-05	236.36
1.33813	0.00067	0.003	5.05E-05	223.28
1.42677	0.00081	0.002	4.47E-05	197.66
1.38266	0.00069	0.002	3.46E-05	153.25
1.36991	0.00082	0.003	4.52E-05	200.16
1.34262	0.00076	0.003	4.28E-05	189.31
1.4196	0.00097	0.003	4.48E-05	198.07
1.33833	0.00061	0.003	3.83E-05	169.51

Table A27. Partition coefficient of NIBA in cellulose insulation

	Sample ID	Weight (w/o ins) [1]	Weight (w/ ins) [2]	Weight (of ins) [2-1]	Weight (after) [3]
<b>Natural Fiber</b>	M16	1.06954	1.78603	0.71649	1.82608
	M17	1.09315	1.86522	0.77207	1.90794
	M18	1.08242	1.88966	0.80724	1.93475
	M19	1.08213	1.83143	0.7493	1.87316
	M20	1.06849	1.91852	0.85003	1.96292

Weight (equilibration)	Δ Weight (g)	Uptake (g/g)	Cins	K
1.83691	0.05088	0.071	5.04E-03	22283.32
1.91719	0.05197	0.067	4.77E-03	21122.19
1.94385	0.05419	0.067	4.76E-03	21064.90
1.88394	0.05251	0.070	4.97E-03	21990.20
1.97657	0.05805	0.068	4.84E-03	21429.44

Table A28. Showing the parameters for accumulation model sample U1 in cellulose

$C_{air}$	0.49	2.99	$mg/m^3$
$C_0$		0	$mg/m^3$
D		7.62E-07	$m^2/sec$
$\epsilon_b$		0.95	
K		0	$mg/mg$
$\rho$		0	$mg/m^3$
K'		21578	$K*\rho$
L		0.01	M
d		0.1	M
a		3.53E-08	1/sec

Table A29. Showing accumulation model sample U1 in cellulose insulation

Days	time,sec	$C_{(cavity),}$ $mg/m^3$			$mg/m^2$	Grams accumu- lated	ppb
0	0	0.00	0	0.00	0	0	0
1	86400	0.01	0	0.01	20	3	1
2	172800	0.02	0	0.02	39	6	3
3	259200	0.03	0	0.03	59	10	4
4	345600	0.04	0	0.04	78	13	6
5	432000	0.05	0	0.05	98	16	7
6	518400	0.05	0	0.05	117	19	9
7	604800	0.06	0	0.06	136	22	10
8	691200	0.07	0	0.07	155	25	12
9	777600	0.08	0	0.08	175	28	13
10	864000	0.09	0	0.09	194	32	15
11	950400	0.10	0	0.10	213	35	16
12	1036800	0.11	0	0.11	232	38	18
13	1123200	0.12	0	0.12	251	41	19
<b>14</b>	<b>1209600</b>	<b>0.12</b>	<b>0</b>	<b>0.12</b>	<b>269</b>	<b>44</b>	<b>20</b>

Table A30. Showing the parameters for accumulation model sample P1 in cellulose

$C_{air}$	2.99	mg/m <sup>3</sup>
$C_0$		mg/m <sup>3</sup>
D	2.18E-07	m <sup>2</sup> /sec
$\epsilon_b$	0.95	
K		mg/mg
$\rho$		mg/m <sup>3</sup>
K'	21578	K*rho
L	0.01	m
d	0.1	m
a	1.01E-08	1/sec

Table A31. Showing accumulation model sample P1 in cellulose insulation

Days	$C_{(cavity)}$ , mg/m <sup>3</sup>			mg/m <sup>2</sup>	Grams accumu- lated	ppb
0	0.000	0.000	0.000	0		0.00
1	0.003	0.000	0.003	6	0.92	0.43
2	0.005	0.000	0.005	11	1.83	0.86
3	0.008	0.000	0.008	17	2.75	1.28
4	0.010	0.000	0.010	22	3.67	1.71
5	0.013	0.000	0.013	28	4.58	2.14
6	0.016	0.000	0.016	34	5.49	2.56
7	0.018	0.000	0.018	39	6.41	2.99
8	0.021	0.000	0.021	45	7.32	3.41
9	0.023	0.000	0.023	50	8.23	3.84
10	0.026	0.000	0.026	56	9.14	4.26
11	0.029	0.000	0.029	62	10.05	4.69
12	0.031	0.000	0.031	67	10.96	5.11
13	0.034	0.000	0.034	73	11.87	5.54
<b>14</b>	<b>0.036</b>	<b>0.000</b>	<b>0.036</b>	<b>78</b>	<b>12.77</b>	<b>5.96</b>

Table A32. Showing the parameters for re emission model, sample U1 in cellulose

$C_{cavity}$	0.49	0.124861	$mg/m^3$
$C_{air}$			$mg/m^3$
D		7.62E-07	$m^2/sec$
$\epsilon_b$		0.95	
K		0	$mg/mg$
$\rho$		0	$mg/m^3$
K'		21578	$K*\rho$
L		0.01	m
d		0.1	m
A		163	$m^2$
V		326	$m^3$
Q		0.0139	$m^3/sec$
b		1.86E-08	1/sec

Table A33. Showing reemission for sample U1 in cellulose insulation

Days	Years	time, sec	C(air), $mg/m^3$	ppb
0	0	0	0.059	9.67
365	1	31536000	0.033	5.37
730	2	63072000	0.018	2.98
1095	3	94608000	0.010	1.66
1460	4	126144000	0.006	0.92
1825	5	157680000	0.003	0.51
2190	6	189216000	0.002	0.28
2555	7	220752000	0.001	0.16



Table A34. Showing the parameters for re emission model, sample P1 in cellulose

$C_{cavity}$	0.0363	$mg/m^3$
$C_0$		$mg/m^3$
D	2.18E-07	$m^2/sec$
$\epsilon_b$	0.95	
K		$mg/mg$
$\rho$		$mg/m^3$
$K'$	21578	$K*\rho$
L	0.01	m
d	0.1	m
A	163	$m^2$
V	326	$m^3$
Q	0.0139	$m^3/sec$
b	8.04E-09	1/sec

Table A35. Showing reemission for sample P1 in cellulose insulation

Days	Years	time,sec	$C_{(air)_3}$ $mg/m$	ppb
0	0	0	0.007	1.21
365	1	31536000	0.006	0.94
730	2	63072000	0.004	0.73
1095	3	94608000	0.003	0.57
1460	4	126144000	0.003	0.44
1825	5	157680000	0.002	0.34
2190	6	189216000	0.002	0.26
2555	7	220752000	0.001	0.21
2920	8	220752001	0.001	0.16

Table A36. Showing the parameters for accumulation model, sample U1 in fiberglass

$C_{air}$	0.49	2.99	mg/m <sup>3</sup>
$C_0$		0	mg/m <sup>3</sup>
D		7.62E-07	m <sup>2</sup> /sec
$\epsilon_b$		0.95	
K		0	mg/mg
$\rho$		0	mg/m <sup>3</sup>
K'		200	K*rho
L		0.01	m
d		0.1	m
a		3.79E-06	1/sec

Table A37. Showing accumulation model sample U1 in fiberglass

Days	t,sec	$C_{(cavity)}$ , mg/m <sup>3</sup>			mg/m <sup>2</sup>	grams accumu- lated
0	0	0	0	0		
1	86400	0.83	0	0.83	17	2.73
2	172800	1.44	0	1.44	29	4.70
3	259200	1.87	0	1.87	38	6.12
4	345600	2.18	0	2.18	44	7.14
5	432000	2.41	0	2.41	48	7.88
6	518400	2.57	0	2.57	52	8.41
7	604800	2.68	0	2.68	54	8.79
8	691200	2.77	0	2.77	56	9.07
9	777600	2.83	0	2.83	57	9.27
10	864000	2.87	0	2.87	58	9.41
11	950400	2.90	0	2.90	58	9.51
12	1036800	2.93	0	2.93	59	9.59
13	1123200	2.94	0	2.94	59	9.64
<b>14</b>	<b>1209600</b>	<b>2.96</b>	<b>0</b>	<b>2.96</b>	<b>59</b>	<b>9.68</b>

Table A38. Showing the parameters for accumulation model, sample P1 in fiberglass

$C_{air}$	2.99	mg/m <sup>3</sup>
$C_0$		mg/m <sup>3</sup>
$D$	2.18E-07	m <sup>2</sup> /sec
$\epsilon_b$	0.95	
$K$		mg/mg
$\rho$		mg/m <sup>3</sup>
$K'$	200	K*rho
$L$	0.01	m
$d$	0.1	m
$a$	1.08E-06	1/sec

Table A39. Showing accumulation model sample P1 in fiberglass

Days	t,sec	$C_{(cavity),}$ mg/m <sup>3</sup>			mg/m <sup>2</sup>	grams accumu- lated
0	0	0.00	0	0.00	0	
1	86400	0.27	0	0.27	5	0.88
2	172800	0.51	0	0.51	10	1.67
3	259200	0.73	0	0.73	15	2.40
4	345600	0.93	0	0.93	19	3.06
5	432000	1.12	0	1.12	22	3.66
6	518400	1.29	0	1.29	26	4.21
7	604800	1.44	0	1.44	29	4.71
8	691200	1.58	0	1.58	32	5.17
9	777600	1.70	0	1.70	34	5.58
10	864000	1.82	0	1.82	37	5.96
11	950400	1.92	0	1.92	39	6.30
12	1036800	2.02	0	2.02	41	6.61
13	1123200	2.11	0	2.11	42	6.90
<b>14</b>	<b>1209600</b>	<b>2.19</b>	<b>0</b>	<b>2.19</b>	<b>44</b>	<b>7.16</b>

Table A40. Showing the parameters for re emission model, sample U1 due to fiberglass

$C_{cavity}$	0.49	2.96	$mg/m^3$
$C_{air}$			$mg/m^3$
D		7.62E-07	$m^2/sec$
$\epsilon_b$		0.95	
K		0	$mg/mg$
$\rho$		0	$mg/m^3$
K'		200	$K*\rho$
L		0.01	m
d		0.1	m
A		163	$m^2$
V		326	$m^3$
Q		0.0139	$m^3/sec$
b		2.00E-06	1/sec

Table A41. Showing reemission for sample U1 in fiberglass insulation

Days	time, secs	C(air), $mg/m^3$	ppb
0	0	1.40	228.97
10	86400	0.25	40.61
20	172800	0.04	7.20
30	259200	0.01	1.28
40	345600	0.00	0.23
50	432000	0.00	0.04
60	518400	0.00	0.01

Table A42. Showing the parameters for re emission model, sample P1 due to fiberglass

$C_{cavity}$	2.19	mg/m <sup>3</sup>
$C_0$		mg/m <sup>3</sup>
D	2.18E-07	m <sup>2</sup> /sec
$\epsilon_b$	0.95	
K		mg/mg
$\rho$		mg/m <sup>3</sup>
K'	200	K*rho
L	0.01	m
d	0.1	m
A	163	m <sup>2</sup>
V	326	m <sup>3</sup>
Q	0.0139	m <sup>3</sup> /sec
b	$8.64 \times 10^{-7}$	1/sec

Table A43. Showing reemission for sample P1 in fiberglass insulation

Days	time, secs	C(air), mg/m <sup>3</sup>	ppb
0	0	0.45	73.05
10	86400	0.21	34.63
20	172800	0.10	16.42
30	259200	0.05	7.78
40	345600	0.02	3.69
50	432000	0.01	1.75
60	518400	0.01	0.83

Table A44. Daily intake due to inhalation for cellulose insulation and sample P1

Year s	C(air),mg/ m <sup>3</sup>	ppb	adult male,µg/kg /day	adult fe- male,µg/kg/d ay	child,µg/kg/ day
0	0.0083	10.857	0.63	0.56	3.27
1	0.0064	6.031	0.56	0.50	2.90
2	0.0050	3.350	0.43	0.39	2.25
3	0.0039	1.861	0.34	0.30	1.75
4	0.0030	1.034	0.26	0.23	1.36
5	0.0023	0.574	0.20	0.18	1.05
6	0.0018	0.319	0.16	0.14	0.82
7	0.0014	0.177	0.12	0.11	0.63
8	0.0011	0.098	0.09	0.08	0.49
9	0.0008	0.055	0.07	0.07	0.38
10	0.0007	0.030	0.06	0.05	0.30
11	0.0005	0.017	0.04	0.04	0.23
12	0.0004	0.009	0.03	0.03	0.18
13	0.0003	0.005	0.03	0.02	0.14
14	0.0002	0.003	0.02	0.02	0.11
15	0.0002	0.002	0.02	0.01	0.08
16	0.0001	0.001	0.01	0.01	0.06
17	0.0001	0.000	0.01	0.01	0.05
18	0.0001	0.000	0.01	0.01	0.04
19	0.0001	0.000	0.01	0.01	0.03
20	0.0001	0.000	0.00	0.00	0.02

Cumulative dose for 20 years	adult male	adult female	child
Micro grams	1136	1007	5893
Grams	1	1	6

Table A45. Daily intake due to inhalation for cellulose insulation and sample U1

Years	C(air),mg/ m <sup>3</sup>	ppb	adult male,µg/kg/d ay	adult fe- male,µg/kg/day	child,µg/kg/d ay
0	0.0662	10.857	5.03	4.46	26.09
1	0.0368	6.031	3.91	3.47	20.29
2	0.0204	3.350	2.17	1.93	11.27
3	0.0113	1.861	1.21	1.07	6.26
4	0.0063	1.034	0.67	0.59	3.48
5	0.0035	0.574	0.37	0.33	1.93
6	0.0019	0.319	0.21	0.18	1.07
7	0.0011	0.177	0.11	0.10	0.60
8	0.0006	0.098	0.06	0.06	0.33
9	0.0003	0.055	0.04	0.03	0.18
10	0.0002	0.030	0.02	0.02	0.10
11	0.0001	0.017	0.01	0.01	0.06
12	0.0001	0.009	0.01	0.01	0.03
13	0.0000	0.005	0.00	0.00	0.02
14	0.0000	0.003	0.00	0.00	0.01
15	0.0000	0.002	0.00	0.00	0.01
16	0.0000	0.001	0.00	0.00	0.00
17	0.0000	0.000	0.00	0.00	0.00
18	0.0000	0.000	0.00	0.00	0.00
19	0.0000	0.000	0.00	0.00	0.00
20	0.0000	0.000	0.00	0.00	0.00

Cumulative dose for 20 years	adult male	adult female	child
Micro grams	5047	4475	26181
Grams	5	4	26

Table A46. Daily intake due to inhalation for fiberglass insulation and sample U1

<b>Day s</b>	<b>C(air),m g/m<sup>3</sup></b>	<b>ppb</b>	<b>adult male,µg/kg/ day</b>	<b>adult fe- male,µg/kg/d ay</b>	<b>child,µg/k g/day</b>
0	1.56622	257.0080 1	119.03	105.54	617.48
10	0.27779	45.58354	70.07	62.13	363.50
20	0.04927	8.08480	12.43	11.02	64.47
30	0.00874	1.43394	2.20	1.95	11.43
40	0.00155	0.25433	0.39	0.35	2.03
50	0.00027	0.04511	0.07	0.06	0.36
60	0.00005	0.00800	0.01	0.01	0.06
70	0.00001	0.00142	0.00	0.00	0.01

<b>Cumulative dose for 70 days</b>	<b>adult male</b>	<b>adult female</b>	<b>child</b>
<b>Micro grams</b>	2042	1811	10593
<b>Grams</b>	2	2	11



Table A47. Daily intake due to inhalation for fiberglass insulation and sample P1

Days	C(air), mg/m <sup>3</sup>	ppb	adult male,µg/kg/day	adult fe- male,µg/kg/day	child,µg/kg/day
0	0.4990	81.88	37.92	33.63	196.73
10	0.2366	38.82	17.98	15.94	93.27
20	0.1122	18.40	23.22	20.59	120.47
30	0.0532	8.73	11.01	9.76	57.12
40	0.0252	4.14	5.22	4.63	27.08
50	0.0120	1.96	2.47	2.19	12.84
60	0.0057	0.93	1.17	1.04	6.09
70	0.0027	0.44	0.56	0.49	2.89
80	0.0013	0.21	0.26	0.23	1.37
90	0.0006	0.10	0.13	0.11	0.65
100	0.0003	0.05	0.06	0.05	0.31
110	0.0001	0.02	0.03	0.02	0.15
120	0.0001	0.01	0.01	0.01	0.07
130	0.0000	0.01	0.01	0.01	0.03
140	0.0000	0.00	0.00	0.00	0.02
150	0.0000	0.00	0.00	0.00	0.01

Cumulative dose for 150 days	adult male	adult female	child
Micro grams	1000	887	5185
Grams	1	1	5

## BIBLIOGRAPHY

- ASHRAE: "Modelling VOC sorption of building materials and its impact on Indoor air quality." [Internet]; 2001. Available from: <http://www.rp.ashrae.biz/page/rp-.pdf>.
- Blondeau P, Tiffonet AL, Allard F, Haghightat F: "Physically based modelling of the material and gaseous contaminant interactions in Buildings: Models, experimental data and future developments." Advances in building research institute. 2008. Volume 2. pp 57 – 93.
- Bruno TJ, Widegren JA, "Gas Saturation Vapor Pressure Measurements of Mononitrotoluene Isomers from (283.15 to 313.15) K." Journal of chemical & engineering data, 2010, Volume 55, pg 159 – 164.
- Cantrell TS et al. "A study of impurities found in methamphetamine synthesized from ephedrine," Forensic Science International, (1988-10). pp. 39–53; Available from: <http://www.erowid.org/archive/rhodium/chemistry/meth.impurities.html>.
- Colorado department of public health and environment. "Clean-up of meth labs guidance document." 2003. Available from: <http://www.cdphe.state.co.us/hm/methlab.pdf>.
- DEA, Maps of Methamphetamine Lab Incidents [Internet]; Available from: [http://www.justice.gov/dea/concern/map\\_lab\\_seizures.html](http://www.justice.gov/dea/concern/map_lab_seizures.html).
- Haghightat F, Lee CS, Ghaly WS. "Measurement of diffusion coefficients of VOCs for building materials: review and development of a calculation procedure." 2002. Indoor air, Vol 12, 81- 91.
- Hunt, D., S. Kuck, and L. Truitt, "Methamphetamine Use: Lessons Learned, final report to the National Institute of Justice," February 2006 (NCJ 209730), available at [www.ncjrs.gov/pdffiles1/nij/grants/209730.pdf](http://www.ncjrs.gov/pdffiles1/nij/grants/209730.pdf).
- Kirchner S., Badey JR., Knudsen HN., Meininghaus R., Quenard D, Sallee H and Saarinen A: "Sorption capacities and diffusion coefficients of indoor surface materials exposed to VOCs: proposal of new test procedures." Proceedings of the 8th International Conference on Indoor Air Quality and Climate – Indoor Air 1999, Edinburgh, Vol. 1, pp. 430 – 435.
- Kleipis NE, Nelson CW, Ott WR, Robinson PJ, Tsang MA, Switzer P, "The National Human Activity Pattern Survey, A resource for assessing exposure to environmental pollutants", Lawrence Berkeley National Laboratory, 1996. Available from: <http://eetd.lbl.gov/ie/pdf/LBNL-47713.pdf>.
- Lstiburek J. "Understanding vapor barriers." Building science digest 106.2006. Issue 106. Available from: <http://www.buildingscience.com/documents/digests/bsd-106->

[understanding-vapor-barriers/files/BSD-106\\_Understanding%20Vapor%20Barriers\\_r2011.pdf](#)

Mackenzie L.Davis, Susan J.Mastern, “Principles of environmental engineering and science”, Second edition, Chapter 6, page 234.

Martyny JW, Arbuckle SL, McCammon Jr. CS, Esswein EJ, Erb N, Van Dyke M. “Chemical concentrations and contamination associated with clandestine methamphetamine laboratories.” *Journal of Chemical Health and Safety*. 2007; 14(4):40-52. Available from: [http://www.njc.org/pdf/Chemical\\_Exposures.pdf](http://www.njc.org/pdf/Chemical_Exposures.pdf).

Martyny JW. “Variability in the Analysis of Wipe Samples Taken for Methamphetamine Contamination,” [Internet]. National Jewish Medical and Research Center; 2008; Available from: <http://health.utah.gov/meth/html/Decontamination/VariabilityReport.pdf>.

Martyny JW. “Methamphetamine stability and recovery in painted drywall Results of initial testing,” [Internet]. National Jewish Medical and Research Center; 2008; Available from: <http://health.utah.gov/meth/html/Decontamination/VariabilityReport.pdf>.

Meninghaus R, Uhde E: “Diffusion studies of VOC mixtures in a building”. *Indoor Air*. 2002. Volume 22. pp.215 – 222.

Meth in air sampling – personal and ambient initial sampling [Internet]. MPCA (Minnesota Pollution Control Agency); Available from: <http://www.pca.state.mn.us/publications/meth-9a.pdf>.

Murnyak. G, Chang HY, “Derivation of health based screening levels for evaluating indoor surface contamination”, *Journal of ASTM international.*, 2011 Vol 8, No.6,.

National methamphetamine threat assessment. United States department of Justice. National Drug intelligence center. Product No: 2010-Q0317-004. 2010. Available from: <http://s3.amazonaws.com/nytdocs/docs/374/374.pdf>.

Roxana ZW, Martyny JW, Kathryn M, Bib G, Lee SN, “Symptoms experienced by law enforcement personnel during methamphetamine lab operations.” *Journal of Occupational and Environmental Science*. 2007; 4, 895 – 902.

Sanderson RS. “Identification of N-Methylbenzylamine Hydrochloride, N-Ethylbenzylamine Hydrochloride, and N-Isopropylbenzylamine Hydrochloride,” *Microgram Journal* January–June 2008; 6(1-2).

- Santos A.P., Wison A.K., Hornung C.A., Rodrigue J.L., "Methamphetamine laboratory explosions: A new and emerging burn injury." *Journal of burn care and rehabilitation* 25, 2004, no 5, pg 228 – 32.
- Salocks CB, Kaley KB, "Clandestine drug labs/methamphetamine," Office of Environmental Health Hazard Assessment. 2003. Volume 1; No 12:  
[http://oehha.ca.gov/public\\_info/pdf/Red%20Phosphorus%20Fact%20Sheet%20Meth%20Labs%2010'03'.pdf](http://oehha.ca.gov/public_info/pdf/Red%20Phosphorus%20Fact%20Sheet%20Meth%20Labs%2010'03'.pdf).
- Salocks CB. "Assessment of Children's Exposure to Surface Methamphetamine Residues in Former Clandestine Methamphetamine Labs." 2007 Dec; Available from:  
<http://health.utah.gov/meth/html/Healthconcerns/CA%20assessment%20of%20children%20health%20risk.pdf>.
- Salocks CB. "Development of a reference dose for methamphetamine." 2009 Feb; Available from:  
<http://health.utah.gov/meth/html/Healthconcerns/CA%20assessment%20of%20children%20health%20risk.pdf>.
- Shu S, Morrison G, "Dynamic solid phase micro extraction sampling for reactive terpenes in the presence of ozone." *Talanta*, 2010.
- Sparks L, Guo Z, Chang J, Tichenor B. "Volatile organic compound emissions from latex paint - Part 1. Chamber experiments and source model development." *Indoor Air*. 1999 Mar; 9(1):10-17.
- Singer BC, Revzan KL, Hotchi T, Hodgson AT, Brown NJ. "Sorption of organic gases in a furnished room." *Atmospheric Environment*. 2004 May; 38(16):2483-2494. St. Peter Former Meth Lab Cleaning and Sealing Effectiveness Study [Internet]. MPCA ; 2007; Available from: <http://www.pca.state.mn.us/publications/meth-19.pdf>.
- Tracey L.Hammon, Susan Griffin."Support for methamphetamine clean up standard in Colorado." *Regulatory toxicology and pharmacology* 48 (2007).102-114.
- Tichenor BA, Guo Z, Dunn JE, Sparks LE, Mason MA. "The Interaction of Vapour Phase Organic Compounds with Indoor Sinks." *Indoor Air*. 1991;1(1):23-35.
- United Nations Office on Drugs and Crimes (UNODC)."Recommended methods for the identification and analysis of Amphetamine, methamphetamine and their ring substituted analogues in seized materials,".2006; Available from:  
<http://www.unodc.org/pdf/scientific/stnar34.pdf>.

- United States Environmental Protection Agency. "Voluntary guidelines for methamphetamine laboratory cleanup." 2008. Available from: [http://www.epa.gov/osweroe1/meth\\_lab\\_guidelines.pdf](http://www.epa.gov/osweroe1/meth_lab_guidelines.pdf).
- United States Department of Housing and Urban Development." The Rehab guide: Exterior Walls, " 1999; Available from: <http://www.huduser.org/Publications/pdf/walls.pdf>
- United States Drug Enforcement Agency, 2011, Available from: [http://www.justice.gov/dea/concern/map\\_lab\\_seizures.html](http://www.justice.gov/dea/concern/map_lab_seizures.html)
- VanDyke M, Erb N, Arbuckle S, Martyny J. "A 24-Hour Study to Investigate Persistent Chemical Exposures Associated with Clandestine Methamphetamine Laboratories," *Journal of Occupational and Environmental Hygiene*. 2009; 6(2):82.
- Wallboard Layering Studies [Internet]. MPCA; 2007; Available from: <http://www.pca.state.mn.us/publications/meth-3.pdf>.
- Weschler C, Nazaroff W. "Semivolatile organic compounds in indoor environments." *Atmospheric Environment*. 2008; 42(40):9018-9040.
- Yang, X.; Chen, Q.; Zhang, J. S.; An, Y.; Zeng, J.; Shaw, C. Y: "A mass transfer model for simulating VOC sorption on building materials". *Atmospheric Environment*, 2001, Vol 35, no. 7, pp. 1291-1299.

## VITA

Nishanthini Vijayakumar Shakila was born on July 5, 1987 in Chennai, India. She received both her primary and secondary education in Chennai, India. While in school she actively participated in science club and won many awards for elocution and painting. She received her Bachelor of Technology degree in Energy and Environmental Engineering from Tamil Nadu Agricultural University, India in 2008. As a part of the degree she worked in MK Raju consultants as undergraduate intern in an energy recovery project from Dec 2007 – Feb 2008. She worked in a consultancy, Renewable Cogen Asia based in India for a year, developing project design documents for clean development mechanism projects. She then started her Master of Science degree in Environmental Engineering at Missouri University of Science and technology, US. In May 2012 she received her Master's degree.